

Review

# Adsorbents, Working Pairs and Coated Beds for Natural Refrigerants in Adsorption Chillers—State of the Art

Piotr Boruta , Tomasz Bujok , Łukasz Mika  and Karol Sztékler \* 

Department of Thermal and Fluid Flow Machines, Faculty of Energy and Fuels, AGH University of Science and Technology, Mickiewicza 30 Av., 30-059 Cracow, Poland; boruta@agh.edu.pl (P.B.); bujok@agh.edu.pl (T.B.); lmika@agh.edu.pl (L.M.)

\* Correspondence: sztekler@agh.edu.pl

**Abstract:** Adsorption refrigeration systems are promising, sustainable solutions for many cooling applications. The operating range and the performance of an adsorption cooling cycle are strongly dependent on the properties of adsorbents, adsorbates, and bed coatings. Therefore, further research and analysis may lead to improved performance of adsorption coolers. In this paper, studies on working pairs using natural refrigerants and the properties of adsorbent coatings were reviewed. The selected working pairs were then thermodynamically characterised and ranked in terms of refrigerant evaporation temperature values. This was found to be a key parameter affecting the applicability of a given adsorbent/adsorbate pair and the value of SCP (Specific Cooling Power), COP (Coefficient of Performance) parameters, which are now commonly used comparison criteria of adsorption chillers. In the analysis of the coating studies, the focus was on the effect of individual parameters on the performance of the cooling system and the effect of using coated beds compared to packed beds. It was found that a fundamental problem in comparing the performance of different cooling systems is the use of different operating conditions during the tests. Therefore, the analysis compares the performance of the systems along with the most important thermodynamic cycle parameters for the latest studies.

**Keywords:** adsorption chiller; adsorption working pairs; coated beds; comparative analysis; natural refrigerants



**Citation:** Boruta, P.; Bujok, T.; Mika, L.; Sztékler, K. Adsorbents, Working Pairs and Coated Beds for Natural Refrigerants in Adsorption Chillers—State of the Art. *Energies* **2021**, *14*, 4707. <https://doi.org/10.3390/en14154707>

Academic Editors: Antonio Zuerro and Gabriele Di Giacomo

Received: 3 July 2021  
Accepted: 29 July 2021  
Published: 3 August 2021

**Publisher's Note:** MDPI stays neutral with regard to jurisdictional claims in published maps and institutional affiliations.



**Copyright:** © 2021 by the authors. Licensee MDPI, Basel, Switzerland. This article is an open access article distributed under the terms and conditions of the Creative Commons Attribution (CC BY) license (<https://creativecommons.org/licenses/by/4.0/>).

## 1. Introduction

In 2018, the total global electricity consumption was 24,738.9 TWh, of which about 2075 TWh was the energy demand for cooling [1]. Moreover, the use of cooling in buildings has been increasing rapidly for several years [1]. This is due to the increasing standard of living and architectural trends observed in the building industry, as well as the increase in average and maximum temperatures from year to year [2]. Therefore, energy efficiency has to be increased as a remedial measure for global warming and increasing energy consumption [1]. In addition, it is also important to note the importance of the refrigeration industry for healthcare. Currently, due to the development of healthcare in underdeveloped countries and the need to store many medicines, the demand for refrigeration in the healthcare sector is increasing worldwide.

The issues raised clearly demonstrate the need to look for alternative refrigeration technologies, which include adsorption refrigeration. Hassan et al. [3] divided adsorption systems into open (air conditioning and dehumidification) and closed (freezing, cooling, and air conditioning). This is a rather conventional division, but it draws attention to the different applications of cold to be obtained and thus the different requirements for refrigerant temperature.

Regarding the use of adsorption chillers to cool buildings, it should be seen as an opportunity to reduce the consumption of non-renewable primary energy and carbon footprint. Adsorption chillers are most commonly used in large facilities such as office

buildings, hotels, hospitals, and manufacturing plants. Chillers that operate at regeneration temperatures in the range of 45–60 °C can be used in hotels and powered by heat recovered from used hot water, while chillers requiring higher desorption temperatures can be used in industrial chillers where waste heat is often in the 60–80 °C range. Refrigerators powered by waste heat enable operation regardless of climate conditions and can be applied in any place where it is possible to utilize waste heat. In addition, apartment blocks and other buildings that heat their buildings with heat from CHP (Combined Heat and Power) plants can be considered. Connecting to a district heating plant involves paying a fixed charge for the capacity demanded regardless of the low heat consumption in summer. Therefore, in these buildings the use of adsorption chillers for air conditioning of apartments can also make economic sense and enable more efficient operation of district heating plants, which have to cope with excess heat in summer. However, it is also possible to use adsorption chillers in buildings where there are no waste heat sources. In every building where there is a possibility to apply solar collectors, it is possible to apply an adsorption chiller, which will use the heat from the solar radiation to cool the building. Adsorption chillers powered by heat from renewable energy sources (mainly solar energy) operate most efficiently in warm climate zones with high solar radiation supply (tropical, subtropical, temperate climate zones). This solution reduces the load on the energy system in the summer and allows efficient cooling without the need for cooling storage. On the other hand, the further development of global healthcare is very often linked to the provision of adequate storage conditions for drugs and vaccines. Here, special attention should be paid to the medical facilities of underdeveloped countries and developing countries, where the lack of widespread access to the electricity grid very often prevents the use of compressor chillers. Taking into account the fact that most of these countries are in African, Asian, and Central American regions, it can be assumed that adsorption cooling systems powered e.g., by solar energy may be a great opportunity for local communities to improve the quality of medical services provided there.

Adsorption systems reduce electricity consumption in refrigeration and air conditioning by exploiting the thermal compression effect of the refrigerant. Therefore, the main driving energy of the adsorption cycle is heat, which can be low-temperature heat or even waste heat. Therefore, adsorption systems are of paramount importance for sustainable use of energy. Additionally, adsorption systems are characterised by a lack of moving parts, which contributes to their silent operation. On the other hand, it should be noted that these systems have been already investigated in the 1980s of the previous century and, despite many studies, are still characterised by low efficiency coefficients and COP and SCP values. This fact often results in limited applicability due to the size of the equipment and cost-effectiveness of the systems used.

However, the use of COP and SCP as evaluation criteria for adsorption chillers does not allow a reliable evaluation and comparison with other appliances. The COP is defined as the ratio of the heat of evaporation of the refrigerant to the heat of preheating and desorption during the operating cycle of the chiller [4]. This formula does not take into account the fact that the unit is powered by, e.g., waste heat, which is simply irretrievably lost in many industrial processes. Furthermore, considering the fact that compressor units are powered by electricity draws attention to another aspect of this comparison, namely, the differences in power and heat quality. Therefore, an actual comparison of the different systems can be made, for example, based on the basis of an exergetic analysis of the adsorption and compressor cycle operation. SCP, on the other hand, is defined as the ratio of the latent heat of vaporisation of the refrigerant to the mass of the adsorbent [4]. This parameter seems to be a more appropriate comparison criterion than COP, since it allows assessment of the mass of the whole system, which is important in the context of the application of the given solutions. Nevertheless, the COP and SCP parameters take into account the heat of vaporisation of the refrigerant, which is directly related to another parameter characteristic of sorption phenomena, namely, uptake. This parameter is used in publications interchangeably with the concept of adsorption rate, and both can

be defined as the mass of adsorbate vapour that has been adsorbed per unit mass of the adsorbent under given conditions. The adsorption rate depends on the temperature, gas pressure and the size of the specific surface area of the adsorbent. Therefore, to compare specific devices, it is necessary to analyse all three of these parameters and pay attention to the desorption temperature and the cold produced. This approach minimises the risk of erroneous conclusions, which can be reached by directly comparing a chiller producing cold for air conditioning purposes with a freezing device. On this basis, attention should be drawn to the need to seek other alternative comparison criteria.

Of course, cooling efficiency is important, especially for the end user who uses the equipment. However, it is necessary to analyse the efficiency of the entire process chains, which consist of several processes linked to different energy carriers. At each stage there are energy or exergy losses, so it is possible to determine the cumulative energy and exergy consumption in the production of a given product/good. In the literature, one can encounter the concept of environmental cost, which refers to the consumption of exergy of non-renewable natural resources but does not consider the impact of CO<sub>2</sub> emissions [5]. Based on this scheme, the approximate efficiency of compressor chillers can be determined, assuming an average EER (Energy Efficiency Ratio) for chillers of 3.5, an average EU electricity generation efficiency of 45%, and an efficiency of energy distribution and transmission of 92% [6]. It can be concluded that compressor chillers have an average primary energy efficiency of 1.5. It should be noted that among the energy sources used in the EU, about 40% of primary energy is generated from fossil fuels, and this rises to more than 70% in some countries. After considering the fact that adsorption chillers can be powered with low-temperature heat, often waste heat or renewable energy sources, a COP of adsorption systems in the range of 0.5 to 0.8 qualifies these units for further research.

When analysing the various comparative parameters of adsorption chillers, it is important to note which component of the system limits the cooling capacity the most. Many components can be mentioned, such as bed heat exchanger, evaporator, condenser, and control system [7], but the first component that affects the cooling cycle is the adsorbent material and its interaction with the adsorbate. Adsorbents, due to their porosity, are characterised by limited heat transport in the bed. It is also worth noting that porosity is a relative concept. From the adsorbent point of view, the pore size is essential (Figure 1), because adsorption occurs most intensively in the micropores and only after they are saturated with adsorbate does it move to mesopores and macropores. Thus, the selection of an optimal adsorbent-adsorbate pair is essential to improve heat and mass transport in the bed [8]. Modifications related to bed design and interference with the thermodynamics of the adsorption process should be implemented for the best materials, according to the authors.

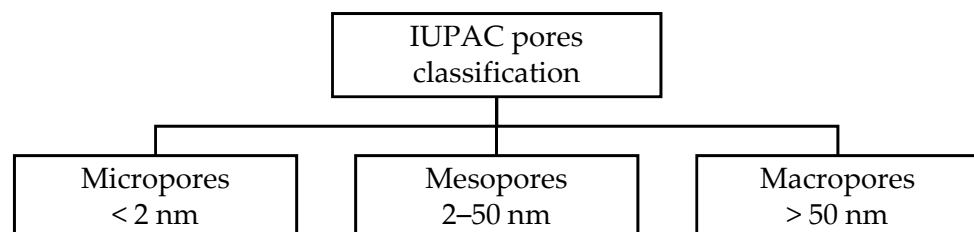


**Figure 1.** IUPAC pore classification in the characterisation of porous materials [9].

Due to the need to develop alternative cooling technologies and to meet the postulates of sustainable development, this article focuses exclusively on the analysis of adsorption working pairs using natural refrigerants (Table 1). Nevertheless, it should be noted that such a trend was already observed in the 19th century, when ammonia or carbon dioxide were used in refrigeration systems. However, the later development of synthetic refrigerants made natural refrigerants less important. It was not until the current regulations concerning ozone-depleting substances [10] that research into alternative refrigerants was

stimulated, because more refrigerants are gradually being phased out, which affects the growing costs of mechanical refrigerators [5].

**Table 1.** Properties of natural refrigerants [11,12].

| Refrigerant        | Critical Temperature [°C] | Critical Pressure [kPa] | Boiling Point <sup>1</sup> [°C] | Heat of Evaporation [kJ/kg] | Thermal Conductivity <sup>2</sup> [W/m·K] | ODP | GWP |
|--------------------|---------------------------|-------------------------|---------------------------------|-----------------------------|---|-----|-----|
| Water <sup>3</sup> | 373.95                    | 22,064                  | 99.97                           | 2256                        | 0.556                                     | 0   | 0   |
| Carbon Dioxide     | 30.98                     | 7377                    | −78.46                          | 379.5                       | 0.015                                     | 0   | 1   |
| Methanol           | 240.20                    | 8220                    | 337.85                          | 1165                        | 0.204                                     | 0   | -   |
| Ethanol            | 240.80                    | 6250                    | 78.2                            | 919                         | 0.171                                     | 0   | -   |
| Propane            | 96.74                     | 4251                    | −42.11                          | 428                         | 0.017                                     | 0   | 11  |
| Isobutane          | 134.66                    | 3629                    | −11.75                          | 367                         | 0.107                                     | 0   | 3   |
| Ammonia            | 132.41                    | 11,357                  | −33.33                          | 1372                        | 0.540                                     | 0   | 0   |

<sup>1</sup> values are given for the liquid at 1 bar pressure. <sup>2</sup> values are given at temperature 0 °C. <sup>3</sup> water vapour is a greenhouse gas, but it is not considered a cause of man-made global warming.

Water as a refrigerant has good thermodynamic properties, but a pressure in the range of 0.6–1.2 kPa is required to obtain chilled water of 0–10 °C [13], which means that a high tightness of the system must be maintained. The group of low-pressure refrigerants also includes methanol and ethanol. On the other hand, carbon dioxide, propane, isobutane, and ammonia have low boiling points at atmospheric pressure. Ammonia enables operation at pressures of 0.5–5 bar, which allows the production of chilled water at temperatures as low as −50 °C [13]. This fact clearly distinguishes this refrigerant from the others. Nevertheless, researchers point to the toxicity of ammonia vapours as a feature affecting the limited number of studies with this refrigerant [14]. It should also be added that an ammonia mixture of 16–27% by volume with air is explosive. Among the refrigerants listed in Table 1, propane is also characterised by explosive properties. For the safety of the cooling system, it must be considered that isobutane, propane, ammonia, methanol, and ethanol are flammable refrigerants. Analysing the data included in Table 1, it should be noted that water has the highest latent heat of the natural refrigerants listed. On the other hand, ammonia, methanol, and ethanol have latent heats 40%, 50%, and 60% lower than water, respectively. Propane, isobutane, and CO<sub>2</sub> all have a latent heat about 80% lower than water. All the refrigerants listed in Table 1 have no ozone depleting effect and are characterised by extremely low GWP. It must therefore be concluded that all the factors listed have a negligible impact on the environment. Thus, when selecting a specific refrigerant, its thermophysical and thermodynamic parameters should be analysed for the specific refrigeration application. There are different adsorbent-natural refrigerant working pairs and, in each application, the one with the best sorption kinetics should be selected.

The currently leading physical, chemical, and composite adsorbents are discussed and the further possible development of each of these material groups is evaluated. In addition, by analysing a number of different adsorbent/adsorbate pairs, the focus is on the applicable comparative criteria of different studies. In the context of adsorbents, the focus is on evaluating pore volume and size, surface development, particle size, and thermal conductivity. On the other hand, only studies that involve the use of natural refrigerants such as water, methanol, ethanol, ammonia, CO<sub>2</sub>, and organic hydrocarbons were selected for the analysis of adsorption working vapours. In addition, the analysis of working adsorption pairs focus on the operating parameters of the refrigeration system. The application of the different working vapours was decided to be divided into three groups: freezing, refrigeration, and air conditioning. Refrigerant evaporation and desorption temperatures have not been analysed as potential comparison criteria of different studies published so far, which affects the difficulty in comparing the different adsorption working pairs. On the other hand, the main aspect of the coating analyses is the influence of the application and design of the adsorbent coatings on the adsorption cycle performance. In this analysis, the basic parameters of the coating structure and the application technology were evaluated

with particular focus on the effects on heat and mass transport. Furthermore, possible gaps in previous research are focused on, with the aim of indicating possible directions for further work related to the search for optimal pairs.

The main objective of this paper is to review, discuss, and compare the research conducted mainly between 2015 and 2021 on the materials currently used in adsorption cooling. Adsorbents as well as coated beds have been considered to improve heat and mass transport efficiency in sorption processes. Consequently, the possibility of improving the COP and SCP performance of the adsorption chiller by modifying the adsorbents was evaluated.

## 2. Adsorbents and Their Influence on a System Performance

As mentioned in the introduction, the adsorption process involves the binding of refrigerant vapours in the pore volume of the adsorbent. Therefore, it should be stated that the adsorbent is the main component of the adsorption refrigeration cycle and is largely responsible for the performance of the refrigeration process. Properties such as sorption kinetics, specific surface area, pore size and pore volume, thermal conductivity, and stability form the basis for evaluating the suitability of a given adsorbent for use in each refrigeration application. In addition, the adsorbent should have the propensity to adsorb large amounts of adsorbate over a narrow temperature range and the ability to desorb rapidly. Moreover, the adsorbent properties should be stable over a wide operating range.

There are many types of adsorbents, both naturally occurring in nature and artificially produced. Generally, adsorbent materials can be divided into three groups:

- physical and novel porous adsorbents;
- chemical adsorbents;
- composite and doped adsorbents [4,15].

Chemical adsorbents are a group of sorption materials that include compounds such as chlorides (e.g., strontium, magnesium, lithium), hydrides (e.g., lithium, calcium), and metal oxides and hydrates of inorganic salts. Chemical adsorbents differ from physical adsorbents because in chemical adsorption there is a strong chemical bond between the adsorbent and the refrigerant. Chemical adsorbents allow higher adsorption capacity, but also require higher desorption temperatures. In addition, chemical adsorbents are also susceptible to swelling and agglomeration phenomena, which generate the problem of clogging of material pores. Therefore, they are rarely used in adsorption systems.

Sharma et al. [16] in their work analysed sorption materials in the form of halide salts such as  $\text{CaCl}_2$ ,  $\text{SrCl}_2$ ,  $\text{MnCl}_2$ , and  $\text{FeCl}_2$ . Of the salts analysed, only two selected salts operate at desorption temperatures of 80–100 °C. Nevertheless, it is the  $\text{CaCl}_2$  salt that shows the best adsorption performance among the analysed compounds. It is characterised by relatively high adsorption capacity at 0.5 g/g and low enthalpy of desorption at 56.59 kJ/mol, which affects the relatively high COP of 0.53.

In general, chemical adsorbents do not play a leading role in the reviewed literature, which includes recent research in the field of materials used in adsorption cooling processes. However, this fact does not exclude their use as admixtures with other adsorbents. Chemical compounds such as strontium chloride [17], calcium chloride [18–20], lithium bromide [21], sodium chloride [20,22], and lithium chloride [20] are currently used as additives in composite materials. The combination of the above-mentioned chemical compounds with classical adsorbents such as SG (Silica Gel), AC (Activated Carbon), and zeolites allows in many cases to improve the heat and mass transport in the material and to increase the adsorption size. At the same time, in many cases, the appropriate choice of the mass proportion of the chemical compound allows to eliminate the negative characteristics of chemical adsorbents, which are the common phenomena of swelling, agglomeration, crystallization, which causes clogging of pores and limiting the size of adsorption. Therefore, Section 2.2 of this paper discusses commonly used composite materials, which can be regarded as an attempt to combine the best properties of physical and chemical adsorbents.

## 2.1. Physical Adsorbents

These adsorbents are used in adsorption chillers and depend on van der Waal's forces to retain the adsorbate. The most widely used physical adsorbents in refrigeration and thus the best studied are activated carbons, zeolites, and silica gels. These materials are often referred to as classical by researchers due to their influence on the development of adsorption refrigeration. Nevertheless, further development of this scientific discipline has led to the identification of novel porous adsorbents such as aluminium phosphate (AlPO), silicoaluminophosphate (SAPO) and metal-organic frameworks (MOFs) [15,23].

### 2.1.1. Activated Carbons

Activated carbons, despite being well known and widely studied materials, are still the basis for further research and this trend is expected to continue. This is due to the fact that, despite the significant development of other adsorbent groups, activated carbons (ACs) provide high sorption dynamics and are characterised by low manufacturing cost. Allouhi et al. [13] pointed out that activated carbons can be produced from various raw materials such as wood, coconut, any nutshells, or coal. When properly treated, these materials exhibit high degree of surface development, the highest among the adsorption materials used. The HDACFs (high-density activated carbon fibres) analysed in Kunit's study [24] are characterised by a surface development of  $3263 \text{ m}^2/\text{g}$ , which is the best among the materials summarized in Table 2. In general, the selected ACs are characterised by good surface development, but vary in a wide range of  $800\text{--}3000 \text{ m}^2/\text{g}$ . Such a high surface development of ACs results in a significant pore volume contribution to the adsorbent mass, which is in the range of  $0.43\text{--}1.85 \text{ cm}^3/\text{g}$ , and the best porosity is characterised by PR KOH4. Analysing the properties of selected activated carbons collected in Table 2, it should be noted that with the increase of surface area, the pore volume in the adsorbent increases. Nevertheless, these two parameters are not sufficient to evaluate the quality of the adsorbent material.

The porosity of the adsorbent is an essential parameter, but the dynamics of the adsorption process is mainly determined by the size of these pores. Physical adsorption occurs first in the micro pores, because they have the strongest interaction with the adsorbate. Only after saturation of the smallest pores, the adsorbate starts to settle in the mesopores. Therefore, the average pore size is an important parameter because it realistically affects the adsorption rate and allows the shape of the sorption curve to be predicted. Brancato et al. [21] analysed the characteristics of five activated carbons: SRD 1352/3, FR20, AP4-60, ATO and COC-L1200, which are characterised by different origins. They found that the pore width of the adsorbent is an important parameter characterising the adsorption capacity of an adsorbent. Therefore, materials such as HDACF [24], Maxsorb III (H2) [18,25,26], and PR KOH4 [27] characterised by very large pore volume ( $1.7\text{--}1.85 \text{ cm}^3/\text{g}$ ) will not necessarily allow high adsorption size, precisely because of the large average pore size. In general, by analysing the average pore size of the materials summarized in Table 2, it should be concluded that ACs are characterised by small pore size, on the order of  $0.5\text{--}0.6 \text{ nm}$ . Nevertheless, treatments that modify activated carbons, such as increasing thermal conductivity by pelletisation, can have a negative effect on pore size. Another treatment is pressing, which can also lead to a reduction in micropores' volume, such as for HDACF material.

A parameter related to porosity is the mentioned thermal conductivity of the adsorbent. Adsorption cooling characteristics require heating of the adsorbent in order to regenerate the bed. Therefore, porosity is important from a heat transport point of view because it slows down the heating of the adsorbent, which is reflected in the very low thermal conductivity values of adsorbent materials. However, this parameter is rarely compiled by researchers e.g., the ACs conductivity of  $0.066 \text{ W}/(\text{m}\cdot\text{K})$  for Maxsorb III (H2) is largely responsible for the low heat transfer efficiency of the bed. On the other hand, HDACF after the granulation process has a much higher thermal conductivity of about  $0.2 \text{ W}/(\text{m}\cdot\text{K})$ ;

nevertheless, as already mentioned, granulation reduces the volume of micropores in the adsorbent.

**Table 2.** Physical properties of activated carbons.

| Ref.       | Adsorbent        | Pore Volume [cm <sup>3</sup> /g] | Thermal Conductivity [W/(m·K)] | BET Surface Area [m <sup>2</sup> /g] | Adsorbent Size [mm] | Average Pore Size [nm] |
|------------|------------------|----------------------------------|--------------------------------|--------------------------------------|---------------------|------------------------|
| [21,28]    | SRD 1352/3       | 0.65                             | -                              | 2613                                 | 0.5–2.0             | 0.56                   |
| [21]       | FR20             | 0.75                             | -                              | 2180                                 | 0.01                | 0.59                   |
| [21]       | AP4-60           | 0.47                             | -                              | 1428                                 | >4.0                | 0.64                   |
| [21]       | ATO              | 0.64                             | -                              | 1745                                 | 0.25–0.6            | 0.59                   |
| [21]       | COC-L1200        | 0.49                             | -                              | 1412                                 | 0.42–1.0            | 0.59                   |
| [22]       | AC               | 0.435                            | -                              | 1237                                 | -                   | -                      |
| [29]       | SRD 1352/3       | 0.65                             | -                              | -                                    | 0.71–1.18           | -                      |
| [30,31]    | CSAC             | 0.43                             | -                              | 804                                  | 0.00022             | 1.76                   |
| [24]       | HDACF            | 1.70                             | 0.162–0.205                    | 3263                                 | 0.018               | 2.10                   |
| [18,25,26] | Maxsorb III (H2) | 1.70                             | 0.066                          | 3045                                 | -                   | 1.12                   |
| [26]       | PR KOH4          | 1.85                             | -                              | 3060                                 | -                   | 1.25                   |
| [32]       | ACM-35.4         | 0.69                             | -                              | 1200                                 | -                   | 2.30                   |

The last parameter in Table 2 is the adsorbent particle size. Analysing the given materials, it should be noted that ACs can be characterised by a size of a few micrometers or millimeters. Brancato et al. [29] in their work investigated the adsorption dynamics for different particle sizes of SRD 1352/3 activated carbon. Their study allows us to conclude that the adsorption capacity decreases as the adsorbent particle size increases. At the same time, the adsorption time increases with decreasing adsorbent particle size. This tendency is due to the fact that intermolecular mass transfer resistances limit the sorption dynamics. On the other hand, for adsorbent grains of increasing size, the sorption kinetics is limited by intramolecular heat and mass transfer. This observation points to the need to analyse the size of the material used, since the use of the same material but with different particle sizes is associated with a change in bed performance over a wide range. Brancato analysed activated carbon particles of 0.21–1.18 mm, which resulted in SCP values in the range of 1.5–2.41 kW/kg [29]. Such values are high, and unprecedented in other publications.

In turn, the fact that activated carbons can have such different particle sizes makes it possible to conduct the analysis of the behaviour of the blends consisting of different particle sizes. In their study, Hamrahi et al. [33] focused on comparing the performance of adsorption cooling based on activated carbon and a mixture of activated carbons. The mixture was obtained by adding different amounts of nano-activated carbon to micro-activated carbon. It was calculated that a 5% addition of nano-AC to the adsorbent improves the adsorption volume and system performance by about 10% with reference to micro-activated carbon. In turn, about 20% proportion of nano-AC can improve the system performance by about 30%. Moreover, the said adsorbent works with regenerative heat, on the order of 70–80 °C.

### 2.1.2. Silica Gels

Referring to the previous studies, it is possible to outline the thesis that silica gels (SGs) are currently a less frequently studied material than, e.g., activated carbons or composite adsorbents. Nevertheless, this material is still widely used in adsorption chillers operating based on solar regenerative heat. This is due to the fact that SGs allow the chiller to operate at low desorption temperatures. Furthermore, as noted by Yaici et al. [34], silica gels as adsorbents are cost-effective and widely available.

Analysing the data in Table 3 [35–41], it should be noted that SGs are characterised by a surface development in the range of 650–1000 m<sup>2</sup>/g and a pore volume in the range of 0.3–0.5 cm<sup>3</sup>/g. Additionally, the silicas listed in Table 3 have pores with an average size of 0.9–3.2 nm. The parameters listed are characterised by lower values than those described by activated carbons. Nevertheless, pore volume and pore size directly affect the heat and mass transfer in the adsorption bed. Therefore, the lower porosity of SGs, relative to other

adsorbents, affects the higher value of the thermal conductivity of silica gels. The thermal conductivity of SGs [38] is 0.72 W/(m·K) and for SG type RD is 0.2 W/(m·K). These values are several times higher than for ACs, so lower temperature heat can be used to regenerate silica gels than to regenerate activated carbon.

**Table 3.** Physical properties of silica gels.

| Ref.    | Adsorbent  | Pore Volume [cm <sup>3</sup> /g] | Thermal Conductivity [W/(m·K)] | BET Surface Area [m <sup>2</sup> /g] | Adsorbent Size [mm] | Average Pore Size [nm] |
|---------|------------|----------------------------------|--------------------------------|--------------------------------------|---------------------|------------------------|
| [35]    | Silica Gel | -                                | 0.72                           | -                                    | 0.26                | -                      |
| [36]    | RD         | 0.462                            | -                              | 827.5                                | 0.7–1.0             | 3.24                   |
| [36,37] | RD-2060    | 0.335                            | -                              | 686.3                                | 0.3–0.7             | 3.19                   |
| [38,39] | RD         | -                                | 0.198                          | -                                    | 0.2                 | -                      |
| [40]    | A-type SG  | 0.491                            | -                              | 997                                  | -                   | 0.90                   |
| [41]    | Silica Gel | 0.375                            | -                              | 650–800                              | 2.0–4.0             | -                      |

Analysing recent studies conducted on silica gels, it should be noted that they focus on the evaluation of the effect of SG particle size on sorption processes. Vodiannitskaia et al. [35] compared different grain sizes of silica gel and addressed the determination of the optimal particle size of the material. It was found that decreasing the particle size affects the porosity of the adsorbent, due to the fact that the micropores become clogged during the material crushing process. The best performance of the system was determined for a particle size 0.5 mm and no significant change in performance was observed with further grinding of the material. Nevertheless, as the particle size increases from 0.5 to 2 mm, SCP decreases by about 10% and reaches a value of 70 W/kg. The same change in adsorbent particle diameter results in a 5% decrease in COP, which is about 0.55. In contrast, Radu et al. [42] investigated the sorption dynamics for two silica gel sizes (0.45 and 0.85 mm) as a function of the number of sorbent layers. The authors found that smaller particles showed better sorption kinetics in monolayer configurations. Moreover, the more layers, the slower the adsorption and desorption processes. The study also determined a negligible effect of increasing the effective diffusivity inside the adsorbent particles on the SCP value. In contrast, decreasing diffusivity significantly decreases the system performance, especially for large adsorbent particle sizes. A similar relationship of decreasing sorption size with increasing particle size was observed by Yaici et al. [34], who investigated the effect of silica gel particle size on adsorption. Their study also confirmed that the use of a silica gel with a smaller size reduces the cycle time. Moreover, the analysis of adsorption curves reveals a relationship that for larger particle sizes the adsorption rate becomes increasingly linear over time.

### 2.1.3. Zeolites

As already mentioned in this chapter, zeolites belong to the group of physical adsorbents that, besides SGs and ACs, can be called classical. Analysing the materials summarised in Table 4, it can be observed that zeolites are characterised by lower pore volume and surface area parameters than the previously described activated carbons and silica gels. The surface area of zeolites is 30–720 m<sup>2</sup>/g and their pore volume is 0.1–0.35 cm<sup>3</sup>/g. However, with a pore size of 0.6–1.2 nm on average and thermal conductivity of 0.02–0.11 W/(m·K), it can be concluded that zeolites are ranked between active carbons and silica gels in terms of sorption properties. It is worth mentioning that zeolites are minerals and there are about 40 naturally occurring zeolites and about four times as many artificially produced ones [13]. This observation influences the fact that these materials continue to be analysed in further studies. In their work, Kayal et al. [43] addressed the study of AQSOA zeolites (Z01 and Z02) using different experimental approaches. It should be noted that these materials are characterised by a significant difference in specific surface area and pore volume parameters. Zeolite Z01 is characterised by a surface area

development of  $132 \text{ m}^2/\text{g}$  and a pore volume of  $0.087 \text{ cm}^3/\text{g}$ . On the other hand, zeolite Z02 is characterised by four times higher values of the given parameters. The authors attributed such significant differences in properties to the difference in ionic radii of  $\text{Fe}^{3+}$  and  $\text{Si}^{4+}$  in the lattice structure of AQSOA-Z01 and AQSOA-Z02, respectively. Furthermore, based on the study, zeolite Z01 is suitable to operate at desorption temperatures below  $65 \text{ }^\circ\text{C}$ , while zeolite Z02 operates more efficiently at  $80 \text{ }^\circ\text{C}$ , which is related to the adsorption curves of these materials. The AQSOA family of zeolites shows very good thermal stability, adequate adsorption charge and high desorption rate.

Similar to SGs, for zeolites also studies are being conducted to evaluate the effect of adsorbent particle size on sorption kinetics. Girník et al. [44] investigated the study of different particle sizes of AQSOA™-FAM-Z02 material. They found that as the zeolite grain size increases, the SCP of the cycle decreases, which is directly related to the increase in adsorption and desorption time for the material with larger particle size. Nevertheless, it should be noted that the adsorption curves for different particle sizes are very similar in shape. Relating these observations to the studies of Yaici et al. [34] and Brancato et al. [29], it should be concluded that SGs, ACs, and zeolites show higher adsorption dynamics for smaller particle sizes. On the other hand, the effect of adsorbent particle size on the shape of the adsorption curve cannot be clearly determined. Girník et al. [45] in another publication also studied the effect of silica gel grain size on the adsorption size of adsorbate. It is worth mentioning that the authors conducted their study on a monolayer of adsorbent, which marginalises the problem related to vapour diffusion of adsorbate, and mainly draws attention to the role of heat transfer. The sorption processes occurring in the adsorbent monolayer cannot be compared with those occurring in a bed consisting of several layers of material, due to the significant difference in the conditions of the process occurrence. Hence, another doubt arises regarding the comparison of different test results. Due to the complexity of the phenomenon in question, individual papers should be carefully collated to avoid drawing incorrect conclusions.

**Table 4.** Physical properties of zeolites.

| Ref.    | Adsorbent    | Pore Volume [ $\text{cm}^3/\text{g}$ ] | Thermal Conductivity [ $\text{W}/(\text{m}\cdot\text{K})$ ] | BET Surface Area [ $\text{m}^2/\text{g}$ ] | Adsorbent Size [mm] | Average Pore Size [nm] |
|---------|--------------|--|---|--|---------------------|------------------------|
| [43,46] | AQSOA-Z01    | 0.071–0.087                            | -   | 132–190                                    | 0.005–0.008         | 1.18                   |
| [43,46] | AQSOA-Z02    | 0.269–0.277                            | -   | 590–718                                    | 0.005               | 1.18                   |
| [46]    | AQSOA-Z05    | 0.07                                   | -   | 187  | -                   | 1.18                   |
| [45]    | AQSOA-FAMZ02 | -                                      | 0.019   | -  | 0.20–0.25           | -                      |
| [38]    | FAM-Z01      | -                                      | 0.113   | -  | 0.2                 | -                      |
| [47]    | AIPO4        | 0.33                                   | -   | 642  | -                   | 0.66                   |
| [47]    | SAPO4        | 0.34                                   | -   | 659  | -                   | 0.66                   |

As for other adsorbents, the adsorption mechanism for zeolites also occurs primarily in micropores. This phenomenon is also of interest to researchers because further understanding of this phenomenon may enable significant development of adsorbents. Fan et al. [48] analysed the interaction of water molecules with the pores of zeolites. The authors found that the interaction potential between the adsorbate and adsorbent can be determined by the isosteric heat of adsorption as a function of AQSOA pore width. Based on their study, they concluded that the interaction between adsorbate molecules and zeolite channels is strongest in the centre of the zeolite channel. The developed relationships indicate the validity of pore size analysis in the adsorbent and can be used to design new types of adsorbents with high kinetics and adsorption size.

However, even the analysis of several parameters does not always allow for unambiguous comparison of adsorbent parameters. Analysing the data collected in Table 4, a conclusion arises that in studies of adsorbents the thermal conductivity of the material is relatively rarely determined, while it is a very significant parameter, as it allows evaluation

of the heat transfer in the material. As a proof of this statement, analyses conducted by Kim's team [47] were quoted for the analysis of the application potential of a new AlPO<sub>4</sub> adsorbent, which was compared with another, already known zeolite SAPO<sub>4</sub>. The AlPO<sub>4</sub> zeolite is characterised by very similar parameters to SAPO<sub>4</sub>. The good adsorption capacity and favourable micro-pore structure are worth mentioning. Despite the very similar sorption properties of these materials, there is a difference in the sorption processes occurring with these sorbents. For AlPO<sub>4</sub>, the desorption process ends at 75 °C, while SAPO<sub>4</sub> continues desorption under these conditions. For SAPO<sub>4</sub>, raising the desorption temperature to 110 °C is most beneficial. This observation highlights the advantage of AlPO<sub>4</sub>, which requires less heat of regeneration, which is directly related to the difference in performance of systems based on these zeolites. On the other hand, it is also necessary to analyse the behaviour of a given material at variable refrigerant regeneration temperatures, as these characterise real refrigeration systems. Mohammed et al. [37], based on their experimental studies, found that silica gel RD-2060 is superior to zeolite AQSOA-Z02 in terms of SCP achieved over the entire range of refrigerant evaporation temperatures analysed. On the other hand, the zeolite in question allows obtaining stable cooling performance over a wide range of adsorption and desorption times. This draws attention to the fact that the values of the COP and SCP parameters are instantaneous and the cooling processes are often characterised by dynamic changes of the individual parameters.

#### 2.1.4. Metal-Organic Frameworks

MOFs are porous materials with a crystalline structure consisting of inorganic metallic nodes and organic ligands. MOFs usually show a steeper adsorption curve than other sorption materials [49]. These materials show very different properties, as the surface area of NU-1000 [49] is less than 2400 m<sup>2</sup>/g, while for (CH<sub>3</sub>)<sub>2</sub>-MOF-801 it is just over 750 m<sup>2</sup>/g. Similar disparities are observed for the pore volume, being in the range of 0.3–1.5 cm<sup>3</sup>/g. As for the average pore size, MOFs are characterised by pore sizes in the range of 0.8–3.5 nm (Table 5).

**Table 5.** Physical properties of MOFs.

| Ref.    | Adsorbent                                | Pore Volume [cm <sup>3</sup> /g] | Thermal Conductivity [W/(m·K)] | BET Surface Area [m <sup>2</sup> /g] | Adsorbent Size [mm] | Average Pore Size [nm] |
|---------|--|----------------------------------|--------------------------------|--------------------------------------|---------------------|------------------------|
| [50,51] | MOF-801                                  | 0.37–0.44                        | -                              | 820–864                              | 0.4–0.5             | 1.08                   |
| [52]    | MIL-101-3                                | 1.12                             | -                              | 2047                                 | 0.42–0.85           | 2.54                   |
| [53]    | NH <sub>2</sub> -MIL-125                 | 0.57                             | -                              | 1305                                 | 0.4–1.8             | -                      |
| [51]    | (CH <sub>3</sub> ) <sub>2</sub> -MOF-801 | 0.30                             | -                              | 756                                  | -                   | 1.10                   |
| [49]    | UiO-66                                   | 0.98                             | -                              | 1508                                 | -                   | 1.06                   |
| [49]    | NU-1000                                  | 1.49                             | -                              | 2362                                 | -                   | 1.43–3.54              |
| [49]    | DUT-67                                   | 0.43                             | -                              | 936                                  | -                   | 0.75                   |

Due to the increasing popularity of these materials, they are the subject of numerous studies as well as review articles. Gordeeva et al. [54] developed a review of the characteristics of adsorbents of MOFs type. In this work, attention was paid to the stability of the materials, i.e., the need for cyclic, long-term operation without degradation of the sorption properties of the material. In addition, an important aspect of the study is the analysis of the stability of MOFs under water contact conditions. The introduction of water into the metal-ligand bond results in the formation of a released cation and a free ligand, that is, it destabilises the material. On this basis, the authors developed a division of MOFs into: thermodynamically stable, high and low kinetic stability and unstable. In turn, Karmakar et al. [55] pointed out that MOFs make it possible to create a material with properties selected specifically for given applications. Recent developments in the field of MOFs are reviewed and the important factors required for the generation of stable MOFs are discussed. Furthermore, the advantages and disadvantages of these materials in relation

to classical adsorbents are discussed. It was concluded, as in the work of Gordeeva [54], that MOFs should be characterised by long-term stability, high thermal conductivity and sorption kinetics, and high adsorption in a narrow temperature range.

With the literature review conducted, newly developed MOFs were highlighted and analysed for adsorption cooling. Han et al. [51] compared classical MOF-801 and MOF-801 with the addition of methyl functional groups. The addition of  $(\text{CH}_3)_2$  improves the micro porosity of the material and its stability. Consequently, the new material shows up to two times faster adsorption kinetics than conventional MOF, and this is reflected in the obtained SCP and COP cycle parameters. Youssef et al. [56] analysed a MOF named Al-Fumarate in their study. The most important conclusion of the study is that this material is insensitive to the reduction of the desorption temperature from 85 to 65 °C. A similar change in desorption temperature for silica gel and AQSOA-Z02 zeolite results in a decrease in SCP by about 90%, while for the MOF analysed it decreases by only about 15%. This fact is particularly important in the context of the application of a given adsorbent in a real system, where the driving heat used can be characterised by varying temperatures. Nevertheless, the AQSOA-Z02 zeolite has an advantage over the other investigated adsorbents in the form of a constant SCP value at a variable evaporation temperature of the medium. This fact, in turn, is important in the aspect of cooling systems, which are characterised by variability of chilled water temperature. As can be seen, the values of the mentioned adsorption, desorption, and refrigerant temperatures are important criteria for comparing different adsorbents. Ma et al. [52] undertook the analysis of MIL-101-3 as a new type of adsorbent for refrigeration applications. Based on the study, it was found that MOF achieves complete desorption at a lower temperature than activated carbons. Moreover, this material has high adsorption capacity and a low desorption temperature of 80–100 °C. In addition, after analysis of 60 cycles of operation, the material was found to be completely stable, based on the lack of degradation of pore volume and specific surface area. Furthermore, Solovyeva et al. [53] analysed a new material from the MOF group, which is  $\text{NH}_2$ -MIL-125. This adsorbent is characterised by desorption temperature (70–90 °C), work stability, and high surface area.

The last parameter that allows the analysis of adsorbents is the grain size of the material. In their work, Solovyeva et al. [57] addressed the study of MOF-801 in the context of evaluating the effect of material grain size on the kinetics of sorption processes. Increasing the particle size of the adsorbent from 0.2 to 0.8 mm results in an increase in adsorption and desorption times by about 300%, for a material arranged as a monolayer. Doubling the number of layers generates an additional increase in sorption time of about 100%. These observations are consistent with the adsorption dynamics of other physical adsorbents. On the other hand, Solovyeva et al. [53] investigating  $\text{NH}_2$ -MIL-125 found that the adsorption size of the adsorbate for grain sizes of 0.2–1.8 mm does not depend on the material size. This is a particularly significant observation as it stands in opposition to the studies described in publications [31,37,48]. On this basis, it should be concluded that the influence of adsorbent particle size on the system performance must be analysed each time.

## 2.2. Composite and Doped Adsorbents

Composite adsorbent materials were developed to optimise the advantages of physical and chemical adsorbents. By design, composite materials are characterised by high adsorption capacity and efficient heat and mass transport. Additives used in composite or doped materials, such as expanded graphite, significantly improve heat and mass transport in the material. It should also be added that the use of additives in adsorbents very often requires the use of a binder to bond the adsorbent and the additive. On the other hand, Seol et al. [40] stated that composite adsorbents are somehow porous matrices impregnated with inorganic salts, so that they show high theoretical adsorption capacity compared to ordinary adsorbents. However, depending on the additives used, there is a risk of eliminating some of the micropores, such that the actual adsorption capacity is not satisfactory. Additionally, the rate of the sorption processes should also be analysed, as

composite materials are often characterised by dynamic changes in this aspect. Therefore, the study of composite materials focuses on both heat and mass transport intensification.

Analysing the data on composite adsorbents collected in Table 6, it should be concluded that this is currently the most studied group of materials in the context of application in adsorption chillers. Since composites are formed by doping one material with another, it can be concluded that there is an unlimited number of new materials that can be created in this way. Based on the literature review conducted, several composite materials have been selected and are currently under investigation.

Younes et al. [58] analysed silica gel-based composites with the addition of EG500 and EG100 (Expanded Graphite) as a material to improve thermal conductivity, which reaches 1.55 W/(mK) and using PVP (polyvinyl pyrrolidone) as a binder. This thermal conductivity value is very high but is associated with a very low COP of the cycle, which is 0.058, so it can be concluded that the proportion of doped graphite in the adsorbent is inappropriate. The authors found that the addition of 2% PVP has a negligible effect on clogging the pores of the adsorbent and thus limiting the adsorption pore volume up to 0.9 cm<sup>3</sup>/g. Nevertheless, this 2% binder is required to prepare a stable composite adsorbent. As the graphite addition increases, the thermal conductivity of the adsorbent increases. Each time 10 wt% graphite is added to SGP (silica gel powder) it generates a 200% increase in the thermal conductivity of the material. However, this effect is accompanied by a decrease in pore volume and composite surface area by about 10%. Therefore, too much graphite addition will decrease the adsorption pore volume in the bed.

Yagnamurthy et al. [59] analysed the thermophysical properties and adsorption characteristics of new composite materials based on Maxsorb III activated carbon. The composite is made by adding natural graphite nanoplatelets and using PVA (polyvinyl alcohol) as a binder. The addition of graphite improves thermal properties while not overly limiting mass transport. In their study, the authors considered different mass proportions of graphite and the results are in line with the study of Younes [58]. As the proportion of graphite in the material increases, the specific surface area and pore volume of the composite decreases. The addition of 40 wt% graphite generates a decrease in the pore volume and specific surface area of the material by about 70% compared to the base AC, while the thermal conductivity increased 64 times, from 0.066 W/(m·K) for the AC to 4.33 W/(m·K) for the composite. The composites proposed by the research team show an inverse relationship between the increase in material conductivity and the amount of refrigerant adsorption. Combining these relationships, it should be concluded that the composites analysed have similar sorption kinetics, which is determined by water vapour diffusion and heat transfer. Thus, the selection of a particular material depends on the specific design of the bed and the given application.

On the other hand, Pal et al. [60] dealt with a composite material based on Maxsorb III activated carbon (similarly to Yagnamurthy et al. [59]), to which graphene nanoplatelets (GNPs) were added and the whole material was consolidated using polyvinyl alcohol (PVA) as a binder. These composites are characterised by a very high surface area of more than 2000 m<sup>2</sup>/g and a large pore volume of the order of 1.0–1.3 cm<sup>3</sup>/g. Moreover, depending on the amount of graphene addition, the developed composite can have up to 23 times better thermal conductivity than the base AC. Based on these studies, one should observe a large variation in the properties of the composite materials depending on the composition. This clearly indicates that further research on composite adsorbents is warranted, as application-specific dedicated materials can be developed. The possibility to work out the structure of the material with specific dominant features such as pore size or volume, thermal conductivity and diffusivity, or surface development allows for concluding that that further development of composite adsorbents will allow an increase in the efficiency of adsorption chillers.

Kumita et al. [24] analysed a composite adsorbent based on activated carbon fibre (ACF) using polytetrafluoroethylene (PTFE) as a binder. The authors found that by consolidating the fibres into larger particles, cooling performance could be improved. The

adsorption and desorption behaviour of the composite HDACF was investigated. The effect of adsorbent density on the adsorption rate was determined. It was observed that the adsorption and desorption rates increase with increasing density of the composite reaching a maximum value for a density of  $380 \text{ kg/m}^3$ . This situation is due to the fact that increasing the density of the composite improves the heat transport in the material. However, further densification of the activated carbon reduces the mass exchange. Thus, it should be concluded that for each material there is a certain limiting density where the balance between heat transfer dynamics and mass exchange in the material allows the maximum adsorption/desorption efficiency to be achieved.

Dzigbor et al. [22] studied composites formed from activated carbon doped with NaCl. They found that doping with NaCl at 30 wt% improves the thermal conductivity of the sorbent by about 25 times. On the other hand, such doping reduces absorption by about 35%. The author speculates that sodium chloride blocked access to the AC micropores, which limits the amount of refrigerant adsorption.

Chen et al. [61] analysed a composite adsorbent based on 13X zeolite and doped with  $\text{CaCl}_2$ . The authors found a reduction in adsorption capacity when trying to improve the thermal conductivity of the material. The answer is proposed by Chen's team [62], who found in an earlier study that such a doped zeolite has a larger pore volume, a better adsorption capacity, and that the increasing proportion of  $\text{CaCl}_2$  is responsible for the increase in pore volume and the development of the material surface area. In general, the study of composite adsorbents impregnated with hygroscopic salts is interesting due to their high affinity for water.

**Table 6.** Physical properties of composite adsorbents.

| Ref. | Adsorbent            | Pore Volume<br>[ $\text{cm}^3/\text{g}$ ] | Thermal<br>Conductivity<br>[ $\text{W}/(\text{m}\cdot\text{K})$ ] | BET Surface<br>Area [ $\text{m}^2/\text{g}$ ] | Adsorbent<br>Size [mm] | Average Pore<br>Size [nm] |
|------|----------------------|---|---|---|------------------------|---------------------------|
| [22] | AC + 20% NaCl        | 0.391                                     | 0.0023  | 1120  | -                      | -                         |
| [22] | AC + 25% NaCl        | 0.365                                     | 0.005   | 1069  | -                      | -                         |
| [22] | AC + 30% NaCl        | 0.331                                     | 0.0054  | 793   | -                      | -                         |
| [61] | 13X/ $\text{CaCl}_2$ | 0.34–0.54                                 | 0.2   | 608–622                                       | 0.002                  | -                         |
| [40] | WSS + 20 wt% LiCl    | 0.368                                     | -   | 149   | -                      | 9.5                       |
| [58] | S2-EG500             | 0.257                                     | 0.34  | 548   | 0.026–0.23             | -                         |
| [60] | AC + 40 wt% GNPs     | 0.958                                     | 1.55  | 1935  | -                      | 2.2                       |
| [58] | SGP                  | 0.284                                     | 0.12  | 601   | 0.1–2.0                | -                         |
| [58] | S3-EG100             | 0.246                                     | 0.28  | 520   | 0.026–0.23             | -                         |
| [63] | S1-PVP               | 0.274                                     | 0.16  | 572   | -                      | -                         |
| [64] | MWCNT/MIL-100(Fe)    | 0.7                                       | -   | -   | 0.005                  | -                         |

Grekoval et al. [20] addressed the development of a new composite based on AA (anodic alumina) that is impregnated with hygroscopic salts ( $\text{CaCl}_2$  and LiCl). The significant adsorption dynamics at the beginning of the cycle (about 150s) should be noted, as well as the subsequent stagnation of adsorption. The reason for this shape of the adsorption curve lies in the structure of the adsorbent. As the process continues, the pores of the material become blocked by the hydrated salt. It should also be added that AA can be characterized by different parameters of pore size and volume, depending on the environment in which it was produced.

Analysing the latest data on adsorbents, it should be concluded that despite many ongoing studies, there is still a great potential for their development. The optimal selection of adsorption materials for a certain refrigeration application allows for the intensification of adsorption and desorption processes.

When comparing different adsorbents' parameters, special attention should be paid to the grain size and average pore size. Analysing the grain size of different adsorbent materials for most of them, a deterioration of sorption dynamics with increasing grain size can be observed. Nevertheless, Mitra et al. [25] analysed the effect of adsorbent particle

size on adsorption dynamics. Based on their analysis, they concluded that it is difficult to unambiguously determine the effect of particle size on the adsorption rate because it is specifically correlated with the bed structure.

In general, all material properties are related to pore size and the amount of energy required to remove adsorbate from the micropores. This is why sorption curves have such different shapes, because there are certain energy levels that must be exceeded to allow adsorption/desorption in a given pore group. Moreover, adsorption always starts in micropores, and only after they are filled do adsorbate molecules move to mesopores, which are characterised by a lower affinity for adsorption of refrigerant, which affects the inhibition of adsorption process [43]. Therefore, how the doping of different materials affects the pore volume should be evaluated each time. Considering the characteristics of the adsorption process, it should be noted that a drastic reduction in the micropore volume significantly reduces the adsorption volume as well as its kinetics. Adsorption occurring in mesopores is characterised by much slower kinetics than that taking place in the smallest spaces of the sorbent. However, this observation does not only apply to composite adsorbents. All procedures involving granulation or fragmentation of adsorbent materials carry the risk of clogging the micropores; therefore, the above-mentioned processes require special attention so that the target effect of improving a given parameter of sorption properties of the material does not have a negative impact on the other properties.

This analysis of sorption materials focuses on comparing the thermodynamic and physical properties of the materials, but other factors such as price and availability of a given adsorbent are also important. Comparing the prices of different sorbents, it can be concluded that ACFs are the cheapest. The next group are zeolites, which are on average two times more expensive than activated carbons. On the other hand, silica gels are about several times more expensive than ACFs [13]. In contrast, the price of MOFs is about \$2300 per 100 g, so this limits its commercial applications [54].

Therefore, the ACs, SGs, zeolites, named as classical materials, despite inferior physical parameters compared to MOFs and composite materials, have lower prices and better availability. It should be noted that ACs can be produced from plant waste, while zeolites or silica gels occur naturally in nature. Therefore, these materials fit better into the concept of sustainable cooling, which should work with natural refrigerants and adsorbents. On the other hand, further such intensive development of MOFs and composite materials may allow overcoming some technological barriers regarding the low efficiency of adsorption refrigeration systems, and this would allow real competition of adsorption chillers with compressor chillers.

### 3. Impact of Coated-Bed Application

Following the selection of appropriate material properties, another factor affecting the efficiency and performance of adsorption cooling systems is the configuration of adsorbent deposition in the bed. In the adsorption cooling process, it is crucial to provide the best possible heat and mass transport to achieve high adsorption and desorption kinetics. Heat transport can be improved essentially in two ways. The first is based on improving the thermal conductivity of the adsorbent and heat exchanger material. The second way is to increase the exchange area by developing the surface area of the heat exchanger elements or modifying the bed structure to reduce the contact thermal resistance. Among the structural configurations of the adsorbent bed, the following bed types can be distinguished: packed beds, consolidated (bonded) beds, coated beds, and hybrid (coated and packed) beds. Currently, packed beds, in which the adsorbent granules are placed in the free space between elements of the heat exchanger, are the most commonly used. This type of bed is characterised by good mass transport, but heat transport is limited by contact thermal resistance and the presence of voids in the boundary layer. The solution to the problem of poor thermal conductivity of packed beds is the application of a binder, which is used in consolidated beds. The material in the consolidated beds is placed in the voids after mixing with the binder, forming a continuous structure after curing. By using the binder,

voids are filled and point thermal contact is replaced by surface contact. A significant disadvantage of this type of bed is that vapour diffusion and thus mass transport is significantly reduced. Therefore, additional steam channels are used. An extension of the consolidated bed concept is coated beds, where the adsorbent material is applied to the heat exchanger elements, forming a thin coat. This solution allows for the positive effects of forming a consolidated boundary layer while maintaining sufficient mass transport. The disadvantage of coated beds is the reduction of the mass content of the adsorbent material in the bed. The last type of beds is hybrid beds, which combine the advantages of coated and packed beds. The concept of building this type of bed is based on the formation of a coating on the exchanger elements and placing granulated adsorbent material in the remaining volume of the bed. The use of coatings improves heat transport and the filling of free spaces with adsorbent has a beneficial effect on the HEX to adsorbent mass ratio.

Table 7 presents recent research related to coated and hybrid beds. Regarding the improvement of heat and mass transport in coated and hybrid beds, special attention should be paid to the coating technique and the basic coating parameters, which include thickness, particle size, structure, and the binder used. These aspects are discussed in the following chapters.

### 3.1. Adsorbent Coating Technologies

Currently, several technologies have been developed to create and apply adsorbent coatings. Wang et al. [15] proposed to classify the techniques for obtaining coatings into ex situ and in situ methods. In ex situ methods, coating formation is based on the application of appropriately selected adsorbent particles with a binder to the surface of the heat exchanger. The in situ method is based on direct crystallisation of adsorbent particles on the heat exchanger surface. When comparing these methods, three main aspects should be considered: heat and mass transport, coating strength, and technological applicability.

In the case of the in situ method, due to the possibility of resigning from adding a binder, the heat transfer resistance between the heat exchanger and the adsorbent is negligible. The lack of binder also has a positive effect on the mass transport, as the binder does not close the adsorbent pores and it is possible to obtain a thinner coating, minimising the resistance to mass transfer to deeper layers of the bed. However, the use of a thinner coating results in the disadvantage of potentially lower chiller performance due to the unfavourable adsorbent to heat exchanger mass ratio.

Coatings made by the ex situ method have better strength properties. The use of a binder increases the flexibility of the coating, which affects the cracking intensity of the coating. Palomba et al. [27] investigated SAPO-34 zeolite coatings obtained by direct crystallisation and dip coating methods for strength. Pull-off test results showed that the coating samples for the in situ method had a mechanical resistance (average) of 0.78 MPa, while the dip-coated samples had a mechanical resistance of 0.82 MPa. In addition, the choice of coating manufacturing method was found to have a greater influence on the fracture mechanism of the coating layers than on the mechanical resistance of the coating. However, it should be noted that the fracture of the coating itself has a significant impact on the fatigue strength and therefore on the durability of the coating.

Ex situ methods are technologically better mastered and easier to scale up for industrial applications. The main advantage of these methods is their wide applicability, i.e., coatings with a binder can be applied to any substrate, only the appropriate selection of the binder is required. Additionally, compared to in situ methods, they usually do not require high temperatures during coating and drying.

Table 7. Research on adsorption coated bed.

| Ref.    | Coating Technology              | Working Pair                            | Coating Thickness [ $\mu\text{m}$ ] | Particle Size [ $\mu\text{m}$ ] | Binder                     | Presented Tests  | Characteristics   |
|---------|---------------------------------|---|-------------------------------------|---------------------------------|----------------------------|--|---|
| [27,65] | dip-coating                     | SAPO-34/water in situ                   | tens of microns<br>100–200          | -                               | -                          | MacBain test (uptake); pull-off test; CFD simulation   | conceptual studies of a coated exchanger based on graphite plates; in situ coatings have lower mechanical strength; in situ coatings have better adsorption properties  |
| [65]    | -                               | polymer (super desiccant polymer)/water | 100–300                             | -                               | -                          | simulations based on analytical model  | a simulation study of the effect of geometric parameters on the performance of an adsorbent-coated bed chiller; there is an optimal adsorbent coating thickness for a given COP value and cycle length; SCP is always larger for smaller coating thicknesses; |
| [66]    | coated with Zehntner applicator | SAPO-34/water                           | 60–460                              | -                               | 2-hydroxyethyl ether       | isochoric temperature step; heat of adsorption (calculated); isochoric equilibrium sorption curve; water uptake(calculated)  | experimental study on the effect of mass transport on system performance; mass transfer limitation is independent of coating thickness; binder contribution and particle size affect inter-molecular mass transfer  |
| [67]    | -                               | SG/water                                | 1500                                | -                               | epoxy resin                | LFM method (thermal diffusivity); CFD simulation   | the numerical analysis of heat transfer of coated and packed adsorption bed; the use of adsorbent coating intensifies heat transfer   |
| [68]    | dip-coating                     | SAPO-34/water                           | 100                                 | -                               | N-propyl trimethoxy-silane | SEM (coating morphology and surface coverage grade); peel, pull-off, impact and microhardness tests (mechanical characterization of the coating); thermogravimetric method (uptake, adsorption kinetic); | experimental testing of SAPO-34 coating; Comparison of coated and packed bed; SCP increases after coating application; Coating has a life time of at least 600 cycles   |
| [61]    | -                               | 13X/CaCl <sub>2</sub> /water            | -                                   | -                               | -                          | tests on lab-scale adsorption chiller  | performance studies of a compact dual cooling system with a coated adsorption bed; the coating significantly improves heat transfer; SCP increased by 256%  |
| [69]    | in situ                         | SG/water                                | 1000–3000                           | 70–149;<br>149–250;<br>250–400; | polyvinyl alcohol (PVA)    | breakthrough curves  | the effect of coating thickness and particle size on heat and mass transport was investigated; a thinner coating with larger particles can achieve better mass transfer performance;  |

Table 7. Cont.

| Ref. | Coating Technology  | Working Pair                         | Coating Thickness [μm]  | Particle Size [μm] | Binder   | Presented Tests  | Characteristics  |
|------|---|--------------------------------------|-------------------------|--------------------|--|--|--|
| [70] | dip-coating   | Y zeolite/methanol                   | 10,000                  | up to 35           | bentonite  | tests on lab-scale adsorption chiller  | experimental studies on improving the performance of the adsorption cooling system; the use of coating allows to reduce cycle time and improve SCP   |
| [71] | -   | zeolite/water                        | 4000                    | -                  | alumina gel precipitated in situ                           | simulations based on analytical model  | simulation studies on the effect of adsorbent coating application; coating application improved heat and mass transport properties; effect of coating thermophysical parameters on SCP was investigated  |
| [72] | spray-coating   | WSS/water<br>SG (A)/water            | up to 800<br>up to 1000 | -                  | 10% LDM6680, Celvolit                                      | LFD + gravimetric method (internal and interfacial mass transfer, sorption dynamic)                      | adsorption properties of coatings with WSS and silica gel were investigated experimentally; a method of determining internal and interfacial mass transport was proposed; A-type silica gel showed lower total mass transfer coefficient than WSS  |
| [73] | Combination of sol-gel and electrophoretic deposition techniques. | SiO <sub>2</sub> /Al composite/water | 60,000–150,000          | 0.1–0.83           | -  | SEM (coating morphology); adsorption uptake (volumetric experiments)                                     | experimental study of adsorption properties of a new type of coating obtained by direct deposition of silica on aluminium plates; the influence of technological parameters on the properties of the coating was investigated; an increase in SDS concentration resulted in an increase in particle size |
| [74] | -   | SG(3A)/water<br>SG(RD)/water         | 1300<br>700             | -                  | epoxy; PVA; corn-flour; HEC; gelatin; bentonite; sepiolite | AUTOSORB-1 analyzer (BET surface); HYDROSORB analyzer (adsorption isotherms); FESEM (coating morphology) | experimental study of adsorption properties of silica gel coatings; analysis of the effect of binder selection; improved heat and mass transport allows reduce half-cycle time and simplified exchanger geometry   |
| [75] | Mitsubishi Plastics Method  | AQSOA/water                          | -                       | -                  | -  | tests on lab-scale adsorption chiller  | experimental study of a new coated-bed adsorption cooling system;  |

Table 7. Cont.

| Ref. | Coating Technology | Working Pair                                    | Coating Thickness [μm] | Particle Size [μm]       | Binder        | Presented Tests   | Characteristics   |
|------|--------------------|---|------------------------|--------------------------|---------------|---|---|
| [44] | -                  | ACM-35.4/methanol                               | 800–14,400             | 800–1800                 | PVA           | Volumetric large temperature jump method (adsorption uptake, adsorption isotherms); SCP (calculated)  | experimental study of the effect of adsorbent grain consolidation on the ad-/desorption process; the effects of grain size and film thickness were investigated; the use of a binder accelerates ad-/desorption   |
| [76] | -                  | Y zeolite/water<br>SAPO-34/water                | 102–135<br>230–290     | 4.8 ± 0.3<br>3.69 ± 0.01 | SilRes MP50E  | 3D LSM (size of particles, height profile); thermobalance manufactured by Rubotherm (equilibrium water adsorption characteristics); thermogravimetric method (adsorption of pure powder); LPJ method (kinetic adsorption characteristics) | experimental study on Y zeolite and SAPO-34 based coatings; effect of binder on adsorption process was investigated; implementation of coatings improves performance; hydrothermal stability was studied  |
| [77] | -                  | MOF (CPO-27(Ni))/water<br>AQSOATM FAM-Z02/water | 100<br>-               | -                        | -             | CFD simulation; simulations based on analytical model   | simulation study of tubular AHEx units possessing adsorbent/ copper foam composites; performance for the composite is inferior to that obtained for AQSOATM FAM-Z02 under similar conditions  |
| [78] | -                  | SG/water  | 100                    | 1                        | silica binder | simulations based on analytical model   | simulation studies of adsorption bed based on adsorbent-coated microchannels; 77% improvement in COP over conventional systems using adsorbent-coated microchannels   |
| [79] | -                  | Aluminium fumarate/water                        | 300;<br>400;<br>500    | -                        | -             | simulations based on analytical model   | simulation studies of coated and packed bed; the effects of geometrical and thermophysical parameters were studied; the use of a binder improves thermal contact, thus increasing the effective thermal conductivity  |
| [80] | bar coating        | FAM—Z01   | 50–800                 | 10–300                   | epoxy YDPN    | simulations based on analytical model   | simulation studies of the effects of cycle time, binder, particle size, and coating thickness on the adsorption cooling process; experimental validation of the model was carried out; coating application reduces cycle time; there is an optimal coating thickness for SCP; |

Table 7. Cont.

| Ref. | Coating Technology         | Working Pair                             | Coating Thickness [μm] | Particle Size [μm] | Binder  | Presented Tests   | Characteristics  |
|------|----------------------------|--|------------------------|--------------------|---|---|--|
| [81] | manual coating             | SG/water                                 | -                      | <200;<br>1000      | PVA;<br>Hydroxyethylcellulose;<br>2-Hydroxyethylcellulose | optical microscope (coating morphology); dynamic mass measurement during desorption (uptake)                    | experimental studies of different binder and adsorbent particle sizes configurations; the choice of binder affects the adsorption dynamics   |
| [82] | Mitsubishi Plastics Method | FAM-Z02/water                            | 330                    | -                  | silicon dioxide based binder                              | tests on lab-scale adsorption chiller   | comparative experimental study of coated and packed adsorption bed; an increase in SCP and COP was observed for the coated bed compared to the packed bed  |
| [83] | -                          | SG/water                                 | -                      | -                  | -   | simulations based on analytical model   | simulation studies of hybrid (coated+packed) adsorption bed; application of coated first adsorbent layer and filling the remaining space with granulate eliminates thermal contact resistance and improves SCP and COP   |
| [84] | PST                        | SAPO-34/water (Aluminum fiber composite) | -                      | -                  | silane-based binder                                       | tests on lab-scale adsorption chiller   | experimental studies of a new type of bed based on coated aluminium fibres; a new UA index was developed to compare adsorbents for different boundary conditions   |
| [85] | dip- coating               | SG + FAM-Z02/water                       | -                      | -                  | silane-based binder                                       | tests on lab-scale and full-scale adsorption chiller  | experimental study of a hybrid adsorption bed system (coated + packed); coated bed, packed bed, and two hybrid bed configurations were compared; increase in coating thickness implies a decrease in adsorption dynamics |
| [86] | in situ                    | SG/water                                 | 15–150                 | -                  | -   | thermogravimetric method (uptake); SEM (coating morphology); simulations based on analytical model              | experimental and simulation studies of the system with a coated adsorption bed, the effect of coating thickness was examined; COP and SPC were compared to the system with a packed bed                                  |
| [87] | in situ                    | zeolite X/water                          | up to 100              | -                  | -   | SEM (coating morphology); volumetric method (adsorption isotherm); XRD (crystallinity and phase identification) | experimental studies of adsorbent coating obtained by direct synthesis from solution under microwave heating; the applied coating technique significantly increases the crystallisation index;                           |

The ex situ method of adsorbent application includes several techniques. The simplest technique, which can be used practically only in laboratory conditions when preparing samples for testing, is the two-step bonding technique. First, a binder is applied to the surface and then the adsorbent particles are evenly distributed on the surface. Another approach for application to heat exchangers is the use of an adsorbent slurry containing a binder, a solvent (usually water), which is applied to the exchanger surface and forms a coating when dry. Capri et al. [82] distinguish several slurry application techniques: dip coating, spin coating, spray coating, and droplet coating.

The most common adsorbent coating technique used in research is the dip coating technique. The process of applying the slurry itself involves complete immersion of the substrate (heat exchanger elements) in the slurry vessel. This technique makes it possible to obtain coatings of uniform thickness on components with complex geometry. The disadvantages of this technique include the limitation of the coating thickness and high adsorbent consumption. Another technique for applying coatings to elements with complex geometries is the spray coating technique. This technique is based on the use of a spray head, airbrush or paint gun. This technique requires less slurry compared to the dipping technique, but does raise the problem of penetrating the substrate cavities adequately.

Droplet coating involves the mutual movement of the applicator and substrate, where the applicator delivers successive portions of the suspension in the form of droplets. In this way, material consumption is reduced and, additionally, as in the case of the dipping technique, relatively simple automation of the process is possible.

A similar technique is spin coating. An applicator placed over the substrate feeds the material and the substrate is set in motion by a vortex. As a result of the inertial force, the slurry is properly distributed on the surface. This technique is designed for less complex geometries.

Wang et al. [15] classified in situ methods into reagent-assisted and inert-assisted methods. When using the first type, the reactants for crystallisation of the zeolite layer are also taken up either by partial dissolution of the support or by extraction from an inert support matrix. In contrast, the second type is based on building the zeolite layer from gels or solutions containing all reactants. The in situ method is mainly used to produce coatings of such adsorbents as mesoporous aluminosilicate molecular sieves, zeolites and metal-organic structures (MOFs) [88].

### 3.2. Relevant Coating Parameters

The important parameters describing the structure of the coating include the following: coating thickness, adsorbent grain size, its structure, and the binder used. The primary purpose of introducing coatings is to intensify heat and mass transport, so the above-mentioned parameters were analysed for their influence on these phenomena.

The thickness of the adsorbent coating is a parameter that has received much attention in research [24,39,50,65–67,70,74,76,79,83,84,89,90]. The main factor that determines the coating thickness is the technology used. In the case of direct crystallisation, coatings with thicknesses of tens of microns are usually used. In contrast, methods using binders allow for larger coating thicknesses, i.e., 100–200  $\mu\text{m}$  [27]. The coating thickness has been found to affect the SCP [65,79,80,91]. As the thickness of the adsorption coating decreases, the specific power increases. This is due to the reduction in mass transfer resistance [71], relative thermal resistance, and relative thermal inertia of the heat exchanger [91], leading to increased heat and mass transfer [80]. It should be noted that decreasing coating thickness is also associated with a decrease in adsorbent mass and an increase in the metal-adsorbent mass ratio [79]. This results in a decrease in chiller efficiency. However, because of improvements of the heat transfer for thinner coatings, it is possible to reduce the cycle time, resulting in improved COP. It was found that there is an optimum thickness and it depends on the objective function, i.e., to achieve maximum COP or SCP, under the given conditions, i.e., adsorbent used and exchanger design [76].

The effect of particle size on the adsorption/desorption process in coated beds has not been as widely studied as the coating thickness. However, based on a review of works [66,69,80], relatively large particle sizes are recommended for coated beds. Ammann et al. [66] conducted an experimental analysis of mass and heat transfer during water sorption on SAPO-34 coatings. The main limiting factor was mass transport. A particular mass transport limitation was found when using adsorbent particles with a diameter of less than 10  $\mu\text{m}$ . This is attributed to an increase in the interparticle resistance to steam flow. Similar results were obtained by Duong et al. [80], where the use of particles with diameters between 10  $\mu\text{m}$  and 300  $\mu\text{m}$  was analysed. It was found that decreasing the particle size resulted in an increase in steam flow resistance. It was also observed that smaller adsorbent particles have a positive effect on the COP value. As a result of using adsorbent particles with a diameter of 150  $\mu\text{m}$  instead of 300  $\mu\text{m}$ , a 30% increase in COP value was obtained. The authors relate this phenomenon to an increase in intraparticle mass transport at smaller particle sizes.

The use of binders was determined by the requirement to reduce the contact thermal resistance by filling the free interparticle space and thus increasing the contact area of adsorbent particles with the exchanger elements. It should be noted, however, that the introduction of the coating also leads to a reduction in the mass transport of water vapour, which adversely affects the efficiency of the system. An important issue is also to ensure adequate strength of the resulting coating. On this basis, it is possible to define several criteria that a suitable binder should meet. Li et al. [74] reviewed adsorbent-binder pairs and defined a good binder as one that meets the following criteria: (1) improves heat transport along the exchanger-adsorbent surface path, (2) does not affect or improves vapour uptake, (3) allows the formation of sufficiently strong adhesive bonds between the adsorbent and the metal base, (4) has high mechanical and thermal strength under varying humidity conditions, and (5) is chemically inert with respect to the adsorbent-adsorbate pair. Similar criteria were presented in an analysis by Sztékler et al. [81]. Duong et al. [80] investigated the effect of binder weight percentage in the coating on the adsorption process. The experiment was conducted for 0%, 5%, 10%, and 15% binder content. Increasing the binder content resulted in a decrease in the adsorption rate to 53% for 15% binder content compared to the sample without binder. COP and SCP also decreased with increasing binder content. For samples with 15% binder content there was an up to 20% decrease for COP and up to 55% decrease for SCP. As can be seen, the binder has a negative effect on the performance of the adsorption cooling system, but the authors emphasise that the use of binders is necessary; hence a maximum low binder content should be used. It should be noted that no attention has been paid to in situ methods that do not require the use of a binder, but as described earlier they are technologically more complicated compared to ex situ methods. The binders considered in the study include, among others, organic binders such as epoxy resin [67,74,80], gelatin [74], hydroxyethylcellulose (HEC) [74,81], polyvinyl alcohol (PVA) [44,74,81], corn flour [74] and inorganic ones: bentonite [70,74,90], silane-based binders [68,85], sepiolite [74].

The last parameter considered is the structure of the adsorbent bed, more specifically the proportion and distribution of porosity. High porosity improves uptake but also increases heat transfer resistance. In contrast, low porosity improves heat transfer but reduces adsorption. Therefore, it is necessary to optimise the porosity proportion to ensure adequate heat and mass transport. Li et al. [92] propose a novel approach to the porosity problem i.e., introducing a non-uniform porosity distribution. A simulation study was carried out to analyse the distribution variation along the  $x$ ,  $y$ ,  $z$  directions, where the  $x$ ,  $y$  directions are parallel to the exchanger surface and the  $z$  direction is perpendicular. It was found that the change in porosity along  $x$ ,  $y$  direction leads to deterioration of adsorption and SCP, while a change along the  $z$  direction with an appropriate distribution allows for an improvement in adsorption and SCP. Linear, quadratic and step distributions were investigated. All types of distributions were considered in two variants with increasing and decreasing porosity from the cooling side to vapour side. Stimulation results indicate that

a distribution with increasing porosity from the cooling side to the vapour side is preferred. Additionally, it is desirable that the porosity gradient increases from the cooling side to the steam side. A suitable gradient was obtained for a quadratic porosity distribution. Using a quadratic porosity distribution, an increase in SCP of 9.5% was found compared to a uniform distribution [92].

### 3.3. Impact of Coated-Bed Application—Research Results

In order to properly analyse the effect of using coated beds on the effectiveness and efficiency of the adsorption cooling process, it is necessary to consider cases under identical or comparable conditions, which consist of adsorbent/adsorbate pair, chiller design, exchanger design, and thermodynamic cycle parameters, i.e., the temperature of the chilled water in the evaporator ( $T_{\text{eva}}$ ), cooling water temperature ( $T_{\text{chill}}$ ), heating water temperature ( $T_{\text{heat}}$ ), and cycle time. On this basis, the work was selected, subjected to further analysis, the results of which are summarised in Table 8.

The introduction of an adsorbent coating causes an increase in the specific cooling power. This is due to the intensification of heat transfer by reducing the thermal contact resistance. The reduction of thermal contact resistance is based on increasing the thermal contact between the adsorbent particles and the exchanger elements and reducing the proportion of free space and porosity in the bed volume [79]. The effect of improved heat transport in the bed was found, among others, in the study of Grabowska et al. [67], where the application of the coating allowed for an increase in the average temperature during desorption by 6% compared to a packed bed. Improved heat transfer allows for an acceleration of desorption and adsorption process, resulting in a shorter cycle and thus an increase in power.

For the effect on efficiency and COP, two opposing research results were observed. Some studies showed a decrease in COP after coating [58,71], while some of the review works showed an increase [19,70,82,86]. The reason for the decrease in performance has been linked to the clogging of pores by the binder, thus reducing adsorption capacity and increasing in the metal to adsorbent mass ratio, leading to an increase in losses associated with heating and cooling of the exchanger [79]. Additionally, the use of a binder causes a reduction in vapour flow paths, leading to a reduction in mass exchange. On the other hand, the authors of the studies in which a positive effect of the coating on COP has been reported identify an increase in efficiency due to a shorter chiller cycle and a reduction in the amount of heat extracted during desorption. Therefore, it is necessary to further investigate the influence of coated beds on the adsorption cooling process, especially in terms of their effect on COP.

**Table 8.** Effect of adsorbent coating on adsorption process performance.

| Ref. | Working Pair                 | Bed Type                      | SCP [W/kg]  | COP                  | SCP Change <sup>2</sup> | COP Change <sup>3</sup> | Cycle Time [s]  | T <sub>ads</sub> /T <sub>des</sub> /T <sub>eva</sub> [°C] | Coating Technique          | Type of Research |
|------|------------------------------|-------------------------------|-------------|----------------------|-------------------------|-------------------------|-----------------|---|----------------------------|------------------|
| [68] | SAPO-34/water                | coated packed                 | 675<br>498  | 0.24<br>0.40         | 35.5%                   | −40%                    | 300             | 28/90/15  | dip coating                | experiment       |
| [19] | 13X/CaCl <sub>2</sub> /water | coated packed                 | 377<br>106  | 0.27<br>0.16         | 256%                    | 68%                     | 3060<br>1060    | 28/85/14<br>22/85/14                                      | -                          | experiment       |
| [70] | Y zeolite/methanol           | coated packed                 | 30–60<br>10 | 0.1–0.12<br>0.08–0.1 | 200–500%                | 20–25%                  | 15–20<br>60–120 | 40/90/10  | dip coating                | experiment       |
| [79] | Aluminium fumarate/water     | coated packed                 | 825<br>290  | -<br>-               | 184%                    | -                       | 400             | 22/90/20  | -                          | simulation       |
| [80] | FAM-Z01/water                | coated packed                 | 485<br>354  | 0.454<br>0.504       | 37%                     | −10%                    | 480<br>840      | 30/80/13  | dip coating                | simulation       |
| [82] | FAM-Z02/water                | coated packed                 | 456<br>118  | 0.27<br>0.21         | 286%                    | 28%                     | 600             | 30/90/15  | Mitsubishi Plastics Method | experiment       |
| [83] | SG/water                     | Hybrid <sup>1</sup><br>packed | -<br>-      | 0.70<br>0.67         | -                       | 4.5%                    | -               | -   | -                          | simulation       |
| [86] | Aluminium oxide/water        | coated packed                 | -<br>-      | -<br>-               | 50%                     | 40–70%                  | 30–600          | -   | in situ                    | simulation       |

<sup>1</sup> coated bed in combination with packed bed. <sup>2</sup> change in SCP value of coated bed in comparison with packed bed. <sup>3</sup> change in COP value of coated bed in comparison with packed bed.

#### 4. Adsorption Working Pairs for Different Refrigerant Evaporation Temperatures

The working pair in the adsorption/desorption cycle is a key component of the adsorption cooling system. To ensure high cooling efficiency, the appropriate adsorption working pair should be selected according to the heat source temperature. Then, the appropriate adsorption refrigeration cycle parameters should be considered and selected them according to the application. The application areas and characteristics are different for different working pairs of adsorption refrigeration systems.

In his analysis of the adsorption cycle working pairs, Shmroukh et al. [50] focused on the experimental approach; he determined whether the given studies were experimental, theoretical or simulation. He identified zeolite-water, silica gel-water, and AC-methanol pairs as classical pairs for which the maximum adsorption capacity is about 0.26 g/g; however, recent studies of these classical material pairs have obtained uptakes of 0.5–0.6 g/g [24,36]. On this basis, it can be concluded that further development of classical adsorption pairs is possible. Nevertheless, new adsorption pairs using composite adsorbents and MOFs allow for higher adsorption capacity.

Younes et al. [93] in a compiled review of adsorption material pairs focused on comparing COP and SCP parameters. Based on their review, they found that SCP and COP are mainly determined for ideal refrigeration cycles, so it is difficult to relate them to real systems. Nevertheless, even laboratory values of COP and SCP obtained for specific operating conditions allow for the assessment of the suitability of a given pair in the context of a specific application.

Goyal et al. [94] in their work collected information on solar-powered adsorption systems. They found that solar systems are still not competitive. Manufacturers of such systems struggle to keep their solutions in the market due to technological and economic constraints.

Shabir et al. [95] developed a review of materials used in adsorption chillers, where he compared the physical properties of adsorbents, adsorption equilibrium, and uptake, but nothing was mentioned about the refrigerant evaporation temperature, which significantly affects the COP and SCP of the system. On the other hand, Papakokkinos et al. [96] in their study pointed out the crucial importance of the values of the system operating temperatures. The authors presented software to predict the minimum desorption temperature for adsorption isotherms classified according to IUPAC. They found that the minimum desorption temperature depends on the shape of the adsorption isotherm.

According to the main objective of the paper, adsorption working pairs using natural refrigerants and desorption heat of less than 100 °C were analysed. In addition, according to the authors, different adsorption working pairs should be compared considering a set of three temperatures: refrigerant evaporation, adsorption and desorption. Only the combination of the mentioned temperatures with the COP and SCP parameters allows a reliable evaluation of the given working pairs. Therefore, in Table 9, selected adsorption working pairs with characteristic parameters of the cycle, arranged according to increasing temperature of refrigerant evaporation, are presented to enable comparison of working pairs operating under similar conditions. Nevertheless, the data summarised in Table 9 are characterised by very high variability and even their ordering does not completely solve the mentioned problem. In addition, Palomba et al. [97] in their publication pointed out the need for a simulation framework for their research. In the mentioned paper [97], a model for conducting calculations of adsorption systems was presented. Unfortunately, it is not fully functional since different components of systems are used by different research teams. This affects the difficulty of comparing different research results and, at the same time, constitutes a problem to be solved: how to interpret research conducted under extremely different conditions.

Table 9. Properties of selected adsorption working pairs.

| Ref.  | Adsorbent                     | Adsorbate       | Evaporation Temperature <sup>1</sup> [°C] | Adsorption Temperature [°C] | Desorption Temperature [°C] | Adsorption Pressure [kPa] | Desorption Pressure [kPa] | Uptake [g/g] | SCP [kW/kg] | COP [-] |
|-------|-------------------------------|-----------------|---|-----------------------------|-----------------------------|---------------------------|---------------------------|--------------|-------------|---------|
| [98]  | AC/ENG-TSA                    | Ammonia         | −15                                       | 20                          | 80                          | -                         | -                         | 0.06         | -           | 0.23    |
| [17]  | SRCl <sub>2</sub>             | Ammonia         | −5  | -                           | 130                         | -                         | -                         | -            | -           | -       |
| [99]  | Maxsorb                       | Ethanol         | −5  | -                           | 70                          | -                         | -                         | 1.129        | -           | -       |
| [99]  | ATO                           | Ethanol         | −5  | -                           | 70                          | -                         | -                         | 0.437        | -           | -       |
| [100] | MIL-101                       | Isobutane       | −5  | 30                          | 85                          | 12.5                      | -                         | 02           | 0.022       | -       |
| [100] | AC                            | Isobutane       | −5  | 30                          | 85                          | 125                       | -                         | 01           | 0.006       | -       |
| [52]  | MIL-101-3                     | Ethanol         | −5  | 25                          | 80                          | 0.5                       | -                         | 0.304        | -           | -       |
| [52]  | MIL-101-3                     | Ethanol         | −5  | 25                          | 100                         | 1.1                       | -                         | 0.45         | -           | -       |
| [98]  | AC/ENG-TSA                    | Ammonia         | −5  | 30                          | 124                         | -                         | -                         | 0.124        | -           | 0.262   |
| [29]  | SRD 1352/3                    | Ethanol         | −3  | 25                          | 90                          | 1.266                     | 7.845                     | 0.25         | 1.49        | -       |
| [28]  | SRD 1352/3                    | Ethanol         | −2  | 30                          | 90                          | -                         | -                         | -            | 0.057       | 0.075   |
| [21]  | SRD 1352/3                    | Ethanol         | −2  | 30                          | 90                          | -                         | -                         | 0.151        | -           | 0.55    |
| [21]  | FR20                          | Ethanol         | −2  | 30                          | 90                          | -                         | -                         | 0.103        | -           | 0.47    |
| [21]  | AP4-60                        | Ethanol         | −2  | 30                          | 90                          | -                         | -                         | 0.086        | -           | 0.49    |
| [21]  | ATO                           | Ethanol         | −2  | 30                          | 90                          | -                         | -                         | 0.103        | -           | 0.48    |
| [21]  | COC-L1200                     | Ethanol         | −2  | 30                          | 90                          | -                         | -                         | 0.26         | -           | 0.39    |
| [21]  | SG/LiBr                       | Ethanol         | −2  | 30                          | 90                          | -                         | -                         | 0.162        | -           | 0.64    |
| [101] | AC35                          | Methanol        | −2  | 35                          | 100                         | -                         | -                         | -            | 0.66        | 0.329   |
| [18]  | SG/CaCl <sub>2</sub>          | Water           | 5   | 50                          | 135                         | -                         | -                         | -            | 0.058       | 0.58    |
| [18]  | Maxsorb III (H <sub>2</sub> ) | Ethanol         | 5   | 50                          | 130                         | -                         | -                         | -            | 0.083       | 0.53    |
| [18]  | CAU-3                         | Ethanol         | 5   | 50                          | 115                         | -                         | -                         | -            | 0.056       | 0.54    |
| [57]  | MOF-801                       | Water           | 5   | 30                          | 85                          | 0.9                       | 4.3                       | 0.21         | 1.5         | 0.67    |
| [30]  | CSAC                          | CO <sub>2</sub> | 5   | 25                          | 80                          | 3450                      | -                         | 0.52         | -           | 0.09    |

Table 9. Cont.

| Ref.  | Adsorbent                | Adsorbate       | Evaporation Temperature [°C] <sup>1</sup> | Adsorption Temperature [°C] | Desorption Temperature [°C] | Adsorption Pressure [kPa] | Desorption Pressure [kPa] | Uptake [g/g] | SCP [kW/kg] | COP [-] |
|-------|--------------------------|-----------------|---|-----------------------------|-----------------------------|---------------------------|---------------------------|--------------|-------------|---------|
| [98]  | AC/ENG-TSA               | Ammonia         | 5   | 20                          | 80                          | -                         | -                         | 0.19         | -           | 0.43    |
| [98]  | AC/ENG-TSA               | Ammonia         | 5   | 30                          | 80                          | -                         | -                         | 0.09         | -           | 0.31    |
| [60]  | AC + 40 wt% GNPs         | CO <sub>2</sub> | 5   | 30                          | 80                          | 4000                      | 7000                      | 0.6          | -           | 0.06    |
| [28]  | SRD 1352/3               | Ethanol         | 7   | 30                          | 90                          | -                         | -                         | -            | 0.095       | 0.1     |
| [21]  | SRD 1352/3               | Ethanol         | 7   | 30                          | 90                          | -                         | -                         | 0.235        | -           | 0.63    |
| [21]  | FR20                     | Ethanol         | 7   | 30                          | 90                          | -                         | -                         | 0.143        | -           | 0.53    |
| [21]  | AP4-60                   | Ethanol         | 7   | 30                          | 90                          | -                         | -                         | 0.122        | -           | 0.58    |
| [21]  | ATO                      | Ethanol         | 7   | 30                          | 90                          | -                         | -                         | 0.152        | -           | 0.55    |
| [21]  | COC-L1200                | Ethanol         | 7   | 30                          | 90                          | -                         | -                         | 0.086        | -           | 0.45    |
| [21]  | SG/LiBr                  | Ethanol         | 7   | 30                          | 90                          | -                         | -                         | -            | -           | 0.72    |
| [102] | AQSOA™-FAM-Z02           | Water           | 7   | 35                          | 90                          | 1.23                      | 4.24                      | -            | 1.8         | -       |
| [41]  | SG                       | Water           | 7   | 30                          | 80                          | 1                         | 10                        | -            | 0.0082      | 0.258   |
| [16]  | CaCl <sub>2</sub>        | Ammonia         | 10  | 25                          | 100                         | 616.3                     | 1903                      | 0.68         | -           | 0.38    |
| [16]  | SrCl <sub>2</sub>        | Ammonia         | 10  | 25                          | 100                         | 616.3                     | 2142                      | 0.136        | -           | 0.33    |
| [52]  | MIL-101-3                | Ethanol         | 10  | 25                          | 100                         | 3.15                      | -                         | 0.7          | -           | -       |
| [29]  | SRD 1352/3               | Ethanol         | 10  | 25                          | 90                          | 3.106                     | 10.412                    | 0.25         | 1.51        | -       |
| [53]  | NH <sub>2</sub> -MIL-125 | Water           | 10  | 30                          | 90                          | 1.24                      | 4.28                      | 0.35         | 2.2         | -       |
| [45]  | AQSOA-FAM-Z02            | Water           | 10  | 30                          | 90                          | 1.23                      | 4.24                      | 0.22         | 1.3         | -       |
| [64]  | MWCNT/MIL-100(Fe)        | Water           | 10  | 35                          | -                           | -                         | -                         | 0.65         | 0.455       | -       |
| [102] | AQSOA™-FAM-Z02           | Water           | 10  | 30                          | 90                          | 1.23                      | 4.24                      | -            | 2.9         | -       |
| [38]  | FAM-Z01                  | Water           | 10  | 30                          | 70                          | -                         | -                         | 0.1368       | 0.2795      | 0.59    |
| [38]  | Type-RD silica gel       | Water           | 10  | 30                          | 70                          | -                         | -                         | 0.134        | 0.207       | 0.6128  |
| [26]  | Maxsorb III (H2)         | Ethanol         | 10  | 30                          | 70                          | 3.17                      | 10.55                     | 0.37         | -           | 0.8–0.9 |

Table 9. Cont.

| Ref.  | Adsorbent                                | Adsorbate       | Evaporation Temperature [°C] <sup>1</sup> | Adsorption Temperature [°C] | Desorption Temperature [°C] | Adsorption Pressure [kPa] | Desorption Pressure [kPa] | Uptake [g/g] | SCP [kW/kg] | COP [-] |
|-------|--|-----------------|---|-----------------------------|-----------------------------|---------------------------|---------------------------|--------------|-------------|---------|
| [26]  | PR_KOH4                                  | Ethanol         | 10  | 30                          | 70                          | 3.17                      | 1055                      | 0.45         | -           | 0.8–0.9 |
| [26]  | H2-treated Maxsorb III                   | Ethanol         | 10  | 30                          | 70                          | 3.17                      | 10.55                     | 0.39         | -           | 0.8–0.9 |
| [37]  | AQSOA-Z02                                | Water           | 10  | 30                          | 85                          | -                         | -                         | 0.37         | -           | 0.16    |
| [37]  | RD-2060                                  | Water           | 10  | 30                          | 85                          | -                         | -                         | 0.31         | -           | 0.4     |
| [25]  | Maxsorb III (H2)                         | Ethanol         | 10  | 30                          | 70                          | 3.2                       | 10.6                      | 0.6          | 0.4–0.7     | -       |
| [103] | Silica Gel                               | Ethanol         | 14  | 30                          | 85                          | 1.01                      | 4.2                       | 0.39         | 0.268       | 0.47    |
| [103] | ACF/BCS                                  | Ammonia         | 14  | 30                          | 85                          | 103.4                     | 1334.8                    | 0.62         | 0.245       | 0.92    |
| [103] | ACF/NCS                                  | Ammonia         | 14  | 30                          | 85                          | 284                       | 1303                      | 0.59         | 0.245       | 0.58    |
| [104] | 13X/CaCl <sub>2</sub>                    | Water           | 14  | 31                          | 85                          | -                         | -                         | -            | 0.06        | 0.15    |
| [104] | Silica Gel                               | Water           | 14  | 31                          | 85                          | -                         | -                         | -            | 0.045       | 0.28    |
| [19]  | Zeolite 13X/CaCl <sub>2</sub>            | Water           | 14  | 28                          | 85                          | -                         | -                         | ~0.6         | 0.319       | 0.22    |
| [105] | Silica Gel                               | Water           | 14  | 25                          | 75–80                       | -                         | -                         | 0.38         | 0.075       | 0.42    |
| [19]  | Zeolite 13X/CaCl <sub>2</sub>            | Water           | 14  | 28                          | 85                          | -                         | -                         | -            | 0.319       | 0.22    |
| [46]  | AQSOA-Z01                                | Water           | 14.8                                      | 30                          | 55                          | -                         | -                         | 0.215        | 0.11        | 0.37    |
| [46]  | AQSOA-Z01                                | Water           | 14.8                                      | 30                          | 80                          | -                         | -                         | 0.215        | 0.19        | 0.34    |
| [46]  | AQSOA-Z02                                | Water           | 14.8                                      | 30                          | 55                          | -                         | -                         | 0.29         | 0.06        | 0.22    |
| [46]  | AQSOA-Z02                                | Water           | 14.8                                      | 30                          | 80                          | -                         | -                         | 0.29         | 0.26        | 0.36    |
| [46]  | AQSOA-Z05                                | Water           | 14.8                                      | 30                          | 55                          | -                         | -                         | 0.22         | 0.025       | 0.26    |
| [46]  | AQSOA-Z05                                | Water           | 14.8                                      | 30                          | 80                          | -                         | -                         | 0.22         | 0.028       | 0.17    |
| [51]  | MOF-801                                  | Water           | 14.8                                      | 30                          | 80                          | 1                         | 5                         | 0.15         | 0.54        | 0.47    |
| [51]  | (CH <sub>3</sub> ) <sub>2</sub> -MOF-801 | Water           | 14.8                                      | 30                          | 80                          | 1                         | 5                         | 0.19         | 0.79        | 0.63    |
| [17]  | SRCl <sub>2</sub>                        | Ammonia         | 15  |                             | 180                         | -                         | -                         | -            | -           | -       |
| [30]  | CSAC                                     | CO <sub>2</sub> | 15  | 25                          | 80                          | 3450                      | -                         | 0.52         | -           | 0.1     |
| [38]  | FAM-Z01                                  | Water           | 15  | 30                          | 80                          | -                         | -                         | 0.1368       | 0.397       | 0.5623  |

Table 9. Cont.

| Ref.    | Adsorbent                     | Adsorbate     | Evaporation Temperature <sup>1</sup> [°C] | Adsorption Temperature [°C] | Desorption Temperature [°C] | Adsorption Pressure [kPa] | Desorption Pressure [kPa] | Uptake [g/g] | SCP [kW/kg] | COP [-] |
|---------|-------------------------------|---------------|---|-----------------------------|-----------------------------|---------------------------|---------------------------|--------------|-------------|---------|
| [38]    | Type-RD silica gel            | Water         | 15  | 30                          | 80                          | -                         | -                         | 0.134        | 0.382       | 0.6572  |
| [35]    | Silica Gel                    | Water         | 15  | 30                          | 80                          | 1.5                       | 5                         | 0.21         | 0.068       | 0.53    |
| [35]    | Silica Gel                    | Water         | 15  | 30                          | 80                          | 1.5                       | 5                         | -            | 0.08        | 0.56    |
| [31,40] | CSAC                          | CO2           | 15  | 25                          | 80                          | 3450                      | -                         | 0.56         | -           | 0.06    |
| [40]    | WSS + 20 wt% LiCl             | Water         | 15  | 30                          | 100                         | 1.57                      | -                         | 0.35         | 0.47        | 0.52    |
| [40]    | A-type silica gel             | Water         | 15  | 30                          | -                           | 1.57                      | -                         | 0.14         | 0.4         | 0.46    |
| [106]   | Silica gel 127B               | Water         | 15  | 30                          | 80                          | 2                         | 7.5                       | -            | 0.215       | 0.587   |
| [39]    | Silica gel RD                 | Water         | 15  | 25                          | 85                          | -                         | -                         | 0.16         | 0.16        | 0.7     |
| [105]   | Silica Gel                    | Water         | 18  | 25                          | 75                          | -                         | -                         | 0.38         | 0.074       | 0.39    |
| [33]    | AC                            | Methanol      | 24  | 30                          | 75                          | 20                        | -                         | -            | 0.028       | 0.11    |
| [47]    | AlPO4                         | Water         | 27  | 35                          | 80                          | 1.6                       | 5.6                       | 0.3          | 0.523       | -       |
| [47]    | SAPO4                         | Water         | 27  | 35                          | 80                          | 1.6                       | 5.6                       | 0.3          | 0.423       | -       |
| [22]    | AC                            | Ethanol 99,7% | -   | 24                          | 95                          | 5                         | -                         | 0.7          | 0.085       | 0.1     |
| [22]    | AC + 20% NaCl                 | Ethanol 99,7% | -   | 24                          | 95                          | 5                         | -                         | 0.6          | 0.074       | 0.082   |
| [22]    | AC + 25% NaCl                 | Ethanol 99,7% | -   | 24                          | 95                          | 5                         | -                         | 0.55         | 0.076       | 0.08    |
| [22]    | AC + 30% NaCl                 | Ethanol 99,7% | -   | 24                          | 95                          | 5                         | -                         | 0.45         | 0.055       | 0.076   |
| [22]    | AC                            | Ethanol 60%   | -   | 24                          | 95                          | 5                         | -                         | -            | 0.075       | 0.09    |
| [22]    | AC + 20% NaCl                 | Ethanol 60%   | -   | 24                          | 95                          | 5                         | -                         | -            | 0.123       | 0.121   |
| [22]    | AC + 25% NaCl                 | Ethanol 60%   | -   | 24                          | 95                          | 5                         | -                         | -            | 0.15        | 0.16    |
| [22]    | AC + 30% NaCl                 | Ethanol 60%   | -   | 24                          | 95                          | 5                         | -                         | -            | 0.113       | 0.146   |
| [51]    | AC                            | Ethanol       | -   | -                           | 80                          | -                         | -                         | 0.14         | -           | -       |
| [51]    | AC                            | Ethanol       | -   | 25                          | 120                         | -                         | -                         | 0.189        | -           | -       |
| [107]   | Zeolite 13X/CaCl <sub>2</sub> | Water         | -   | 40                          | 75                          | 0.873                     | 12.352                    | 0.4          | 0.018       | 0.76    |

<sup>1</sup> evaporation temperature given by the adsorption pressure.

### *Studies on Different Adsorption Working Pairs*

Quadir et al. [108] performed research using an adsorption chiller driven by solar heat. The paper points out that many different studies related to the use of solar energy for bed regeneration assume a constant adsorption/desorption cycle time, while the solar input is variable. Therefore, fixed and variable cycle times of the device were compared, knowing that optimal adsorption/desorption times are related to achieving equilibrium adsorbate uptake in the adsorbent. The proposed adaptive cycle adjusts the duration of the sorption processes to the difference between the current and equilibrium uptake taking into account the magnitude of the pressure gradient in the bed. The authors noted that the fixed cycle time is suitable for laboratory conditions, where it allows for high specific cooling power. In real conditions, however, cooling is a dynamic process and cycle times need to be modified. The research conducted allowed for stating that adaptive cycle times improve COP and SCP of the system.

Li et al. [39] evaluated the working steam behaviour of SG RD-type/water at a desorption temperature of 85 °C. They found that reducing the cycle time leads to insufficient heating/cooling of the bed, and this entails a more imbalanced heat transfer. Furthermore, the COP cooling efficiency increases almost linearly with increasing desorption temperature. The authors also concluded that bed porosity analysis should be performed in addition to adsorbent porosity analysis. Different packing of the adsorbent in the adsorption bed leads to porosity grading and changes in cycle efficiency.

Papakokkinos et al. [106] conducted a study of the SG 127B/water working pair, where the desorption energy is supplied by a solar collector system. In this paper, the results of dynamic simulations of the entire adsorption system were analysed. It was found that dynamically varying the cycle time allows for improving the efficiency of the system, and the combination with solar collectors is a way to significantly reduce CO<sub>2</sub> emissions. The analysed system allows for high SCP and COP values of 215 W/kg and 0.59, respectively, which are among the higher values obtained by solar-powered systems.

Seol et al. [40] found that the COP and SCP tend to decrease with increasing adsorption time due to decreasing rate of sorption kinetics. On the other hand, the COP value increases with the cycle time, so it is necessary to optimise the cycle time. From the study, it can also be observed that the WSS + 20 wt% LiCl composite has a COP that is about 5–15% better than the type A silica gel. Similar aspects of the analysis of the appropriate adsorption termination time were analysed by the Velte team [109], who used an experimental approach involving a combination of experiment and computer simulations. An interesting observation is the dependence of uptake on adsorption time. The difference in adsorption time for which the uptake is 80% of the maximum capacity and 90% of the maximum capacity is very significant, about 40–60%, which evidently affects the SCP parameter. In such a system, it is necessary to analyse the process carefully and decide the appropriate time to stop the adsorption process.

Liu's publication [41] analysed similarly the adsorption cycle regenerated by solar heat. An interesting aspect of the study is the focus on the duration of bed heating and pre-cooling. In the analysed system, the pre-cooling takes as long as 120 min. Furthermore, it was found that in the range of adsorption time of 30 min, the desorption time is similar. Nevertheless, the more optimal adsorption time is 45 min, which corresponds to a desorption time of about 28 min. From the point of view of the performance of the whole system, the duration of the whole cycle is important, i.e., the adsorption and desorption times, but also the heating and pre-cooling of the bed. SG was found to be more susceptible to cycle time variations than SAPO-34. This is a very important finding because most often studies focus on evaluating COP and SCP at a specific point. On the other hand, from the point of view of the actual system, a wider range of operation should be analysed, since efficient operation over a wide range of operating parameters is a very important criterion necessary for the commercialisation of adsorption chillers.

The cited studies indicate the need to analyse the refrigeration cycle time. Therefore, when selecting a given adsorbent/adsorbate pair, it is necessary to pay attention to the

properties of these materials, as they have a direct impact on the cycle time. Sah et al. [110] in their study also analysed solutions using only low temperature heat i.e., such systems where the driving energy is solar heat or waste heat. Their study shows that the adsorption rate is proportional to the bed pressure and the desorption rate depends on the size of the pore area occupied by the adsorbate and the activation energy.

Radu et al. [42] pointed out that in general the desorption process occurs more intensively than the adsorption process due to the faster diffusion of the adsorbate vapour at higher temperatures. Similar conclusions are drawn from the work of Chan [19], who also notes that desorption is faster than adsorption due to the fact that the vapour moves faster at higher temperatures and pressures (by virtue of kinetic theory of gases).

Elsheniti et al. [105] focused on the analysis of SG/water pair performance. Based on their analysis of adsorption kinetics, they found that higher evaporation pressure enhances adsorption mass transfer mechanisms in the adsorbent, which affects the achievement of higher uptake values for higher adsorption pressures. The present study also highlighted the need to select the application of a particular device, to determine the temperature of the heat source, which affects the selection of a suitable adsorption working pair for a particular application. It was also found that increasing the chilled water temperature by 4 °C allows for a 25% reduction in cycle time, while maintaining the baseline COP and SCP values.

Since higher adsorption pressure has a positive effect on the adsorption kinetics of refrigerant vapours in the adsorbent, attention should be paid to ammonia as a refrigerant. As mentioned in the introduction, ammonia allows operation at pressures close to or even higher than atmospheric pressure, which seems to be a very advantageous feature of this refrigerant. The study by Xu [98] evaluated the possibility of using ammonia as a refrigerant in deep-freezing processes, with a temperature of  $-25$  °C, a desorption temperature of the order of 75 °C and an adsorption temperature of 40 °C. This system has a very low uptake of 0.02 g/g for  $-25$  °C freezing temperature and 0.28 g/g for 15 °C cooling temperature, respectively. Nevertheless, the desire to achieve a freezing effect with such a low temperature requires a desorption heat of 150 °C. These studies simultaneously highlight the problems associated with the use of ammonia in an adsorption refrigeration system, but also provide insight of the potential applications of ammonia in freezing, which requires further research.

Sinha et al. [103] in their study compared classical SG/water pair and pair using ACF/BCS or ACF/NCS composite material along with ammonia. The systems with ammonia allow better energy conversion, which is important for this system that is driven by heat from solar panels.

On the other hand, Boman et al. [18] in their study focused on evaluating vapour applications from the perspective of heating and cooling. They found that the ammonia/AC vapour is suitable for both heating and cooling, while the ethanol/AC vapour performs very well only in cooling applications. The ethanol/MOF pair analysed shows good performance in a cooling context. This research highlights the fact that there are many variants of adsorbent/adsorbate combinations, and the behaviour of a given working pair within changing operating conditions is highly variable.

Dzigbor et al. [22] analysed the AC + NaCl pair working with ethanol. They found that the AC/ethanol pair had better uptake than the pair using the composite adsorbent, which is also reflected in the COP and SCP parameter values. However, the authors noted that the addition of water to ethanol at 40% of the adsorbate volume generates better heat and mass transport in the adsorbent, resulting in an improvement in SCP for the composite steam of about 100% compared to pure ethanol. This information also indicates an interesting research direction related to the mixing of different natural refrigerants and their effect on adsorption performance.

Tso et al. [104] compared systems operating with different working pairs of SG/water and 13X + CaCl<sub>2</sub>/water. The COP of the system using the composite material is 60% lower than that for the steam with SG. In contrast, under the same conditions, the SCP for the

pair with composite is about 30% higher. This is due to the fact that the analysed composite has worse adsorption kinetics than for silica gel. In addition, the composite component is  $\text{CaCl}_2$ , and chemical adsorbents require more heat for desorption than physical adsorbents.

Han et al. [51] analysed MOF-801 and the same material doped with  $(\text{CH}_3)_2$  ligand. The doped MOF exhibits better COP and SCP parameters than the classical MOF-801 when interacting with water. Nevertheless, both pairs dominate in terms of characteristic parameters over SG type A/water, SG type 3A/water and AQSOA Z01 and Z02 pairs also with water as adsorbate. The uptake for the new MOF is about 25% better than that of the regular MOF. This draws attention to the need for further research related to modifications of already existing very good MOF adsorbents.

In his work [38], Hong studied the sorption dynamics of another zeolite, FAM-Z01, which works with water as an adsorbate. This pair is characterised by a low desorption temperature of about 80 °C and fast sorption kinetics. Compared to SG type RD/water vapour, zeolite vapour has better SCP with similar COP, which allows the construction of more compact chillers. Moreover, zeolite pair after lowering the refrigerant evaporation temperature has a significant advantage over SG pair in terms of 65% better uptake value and 35% higher SCP value, i.e., it can be concluded that zeolite water pair outperforms SG/water pair in terms of the range of optimum operation.

Brancato et al. [21] evaluated the characteristics of different adsorption materials, specifically 5 different activated carbons: SRD 1352/3, FR20, AP4-60, ATO and COC-L1200, which are characterised by very different origins and grain sizes. The pore width of the adsorbent was found to be an important parameter characterising the adsorption capacity of the adsorbent. Based on the comparison of the mentioned activated carbons with the SG/LiBr composite material, it was observed that the value of the regeneration temperature has less influence on the performance of the systems with the composite material than in the case of AC-based systems. It was found that lowering the desorption temperature by 30 °C, generates a decrease in COP for AC by about 65%, and for the composite by about 50%. Furthermore, lowering the ethanol evaporation temperature from 7 to −2 °C generates a decrease in COP of about 10–15% for all analysed operating pairs. The selection of particular cycle temperatures is, next to the already analysed role of cycle time, a very important element in of chiller operation optimisation.

Allouhi et al. [13] in their study were concerned with the search for an optimal working pair for a refrigeration application. They analysed different classical working pairs at different evaporation temperatures of refrigerant. On this basis, it should be concluded that lowering the evaporation temperature by 5 °C generates a decrease in COP by about 15–20% and a reduction in evaporation temperature by 15 °C implies a decrease in COP value by 43–50%. On this basis it can be concluded that for the analysed working pairs AC/methanol, AC/ammonia, AC/ethanol, zeolite/ethanol, and zeolite/water/SG/water, the decrease in COP is directly proportional to the decrease in evaporation temperature of the refrigerant.

Solovyeva et al. [57] estimated the adsorption dynamics of MOF-801 with water as a working pair. The maximum uptake of this pair is reaching about 0.4 g/g. Nevertheless, the tests carried out at a water evaporation temperature of 5 °C allow the adsorption capacity to obtain 0.2 g/g. It was also observed that lowering the desorption temperature from 90 to 75 °C increases the adsorption time by about 80%. The same author in publication [53] analysed the MOF  $\text{NH}_2$ -MIL-125 in cooperation with water. This pair achieved an SCP value of 2.2 kW/kg with a water evaporation temperature of 10 °C. In addition, increasing the desorption temperature from 90 to 110 °C reduces the desorption time by half.

Rogala et al. [111] analysed the SG/water pair in their study. They pointed out the possibility of lowering the desorption temperature from 80 to 60 °C, or even less. However, this treatment lowers SCP and COP by about 65 and 50%, respectively, compared to the higher desorption temperature. Thus, if very low temperature heat is to be used, the temperature in adsorption process should be lowered, preferably below 25 °C.

Similar observations come from the study of Singh's team [30], who presented an analysis of the adsorption kinetics of CSAC/CO<sub>2</sub> vapour. It is worth mentioning that CSAC is derived from coconut shells, i.e., it is a waste material. The authors found that the CO<sub>2</sub> adsorption decreases with increasing adsorption temperature, which is related to the decrease in the bond strength between adsorbate and adsorbent during adsorption. Therefore, to maintain sufficient CO<sub>2</sub> uptake, the adsorption bed should be cooled. In addition, a 15 °C increase in evaporating medium temperature generates a 25% increase in COP and about 50% increase in SCP. The opposite trend is observed for increasing adsorption temperature, since an increase of 15 °C implies a decrease in COP and SCP of about 75%.

Jribi et al. [112] presented an experimental approach, where the first step is to perform experimental measurements that are used to validate the developed CFD (Computational Fluid Dynamics) model. In his study, he addressed the validation of ethanol adsorption model on Maxsorb III. He pointed out the necessity to remove the heat of adsorption because the lack of cooling during adsorption generates a significant decrease in process efficiency.

## 5. Discussion

The results of studies by various authors presented in this paper show a wide variety of working pairs both in terms of materials and working parameters as well as COP and SCP ratios obtained. Some working pairs in adsorption devices may be characterised by low values of COP and SCP and such working parameters that practically exclude their commercial applications.

The figure (Figure 2) shows the dependence of the COP on the SCP, for selected adsorption working pairs listed in Table 9. It should be noted that, according to the criterion imposed when preparing the list, all pairs are characterized by a heat of regeneration not exceeding 100 °C, but they differ in the temperature of evaporation of the refrigerant. Unfortunately, the addition of the third axis on the graph (evaporating temperature of the refrigerant) significantly reduces its readability. Therefore, it was decided to focus on the analysis of the dependence of these two parameters only and to indicate the possible application of the working pair. The working pairs analysed were divided into 3 groups of applications depending on the refrigerant temperature of evaporation ( $T_{\text{eva}}$ ), freezing ( $T_{\text{eva}} < 0$  °C), refrigeration ( $0$  °C  $< T_{\text{eva}} < 15$  °C) and air conditioning ( $T_{\text{eva}} > 15$  °C).

Conducting an analysis of the advantages and disadvantages of each adsorption working pair is not easy, due to the diversity of applications. A given pair may have extremely different operating parameters depending on the values of operating temperatures. Regarding the working pairs with the highest evaporating temperatures that are classified as suitable for air conditioning systems, they have an SCP in the range of 0.4–0.7 kW/kg, with a much lower COP, which is less than 0.5. It is also worth noting that the pairs with the highest  $T_{\text{eva}}$  value are combinations of different adsorbents with water as the adsorbate. This is directly related to the good performance of water as a refrigerant and the lack of need to keep the bed pressure as low as needed as for lower evaporation temperatures. As can be easily seen, the best COP and SCP parameters are characterised by MOF/water pairs, because they have a COP of over 0.6 and SCP of over 0.8 kW/kg. It is also worth mentioning that the MOF-801/water pair [57] operates at an evaporation temperature of 5 °C (for a pressure of 900 Pa) and at a regeneration temperature of 85 °C. These performance and temperature parameters allow for speaking about the validity of using adsorption chillers for cooling purposes. However, the fact that the best COP and SCP values are related to the use of MOFs, which are several to a dozen times more expensive than classical adsorbents, makes these working pairs uncompetitive. The study of different working pairs at  $T_{\text{eva}}$  corresponding to freezing processes is associated with obtaining low values of COP and SCP at the level of a few watts per kilogram. Nevertheless, attention should be paid to the AC35/methanol pair [101], which allows obtaining a COP of 0.33 and an SCP of 0.66, at an evaporation temperature of −2 °C and at a regeneration temperature of 100 °C.

These values indicate great potential for the development of adsorption chillers operating at negative refrigerant evaporation temperatures. Freezing applications, however, involve the use of adsorbates other than water, and currently the most extensively studied working pairs are those using methanol or ethanol.

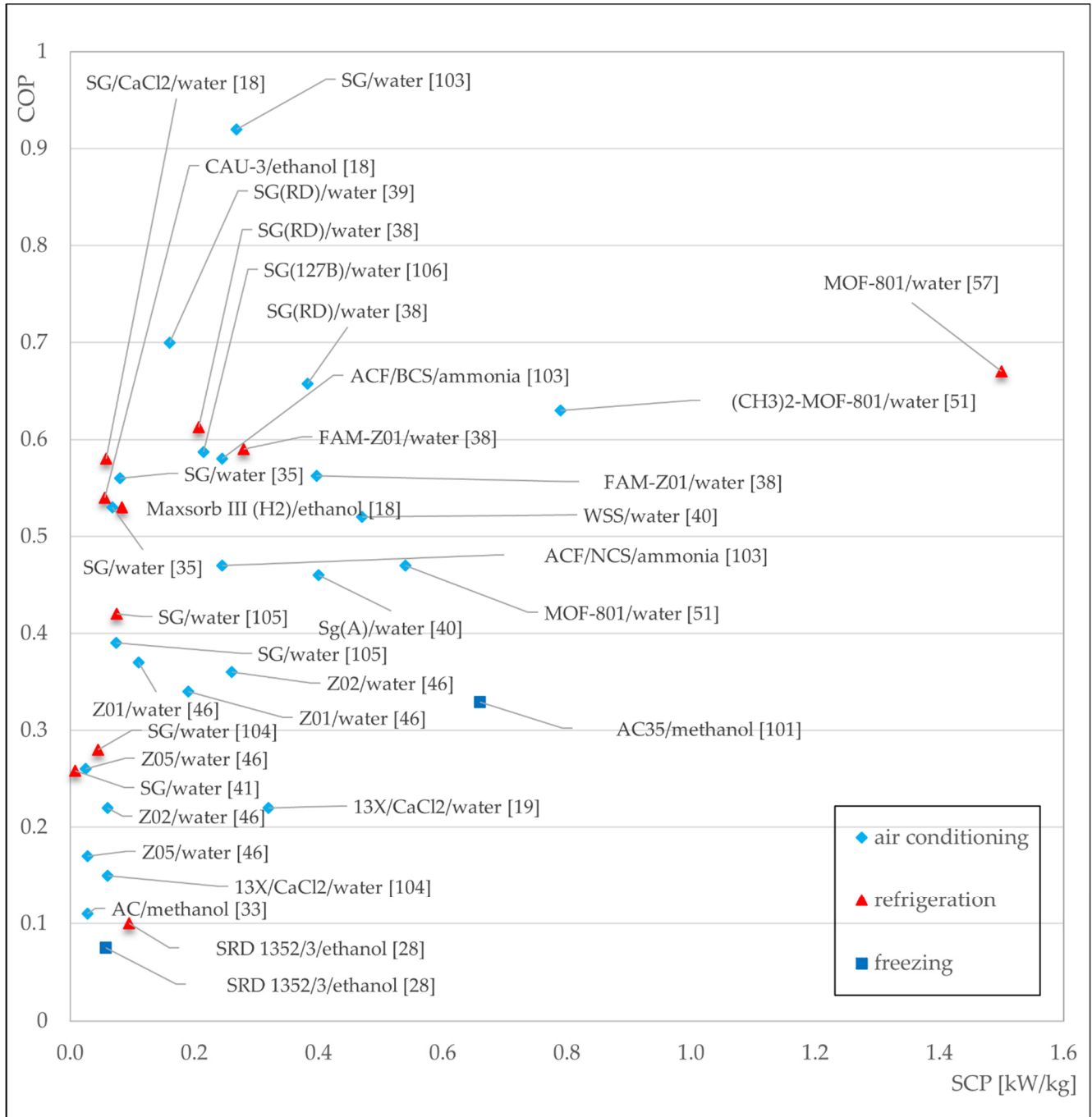


Figure 2. Correlation of the COP parameter on the SCP for different working pairs.

Referring to the data in Table 9 and the conclusions of the selected studies, it should be stated that the selection of the optimal adsorbent/adsorbate pair allows for a significant improvement of the adsorption cycle. Almost every paper has written about the dependence of the increase in COP with increasing adsorption time, which in turn is accompanied by a decrease in SCP. Another element common to all studies is the fact that the values of COP and SCP coefficients increase with increasing the evaporation temperature of the

refrigerant, while the values of these characteristic parameters decrease with decreasing desorption temperature. It can be concluded that the tabular statement in the shape of Table 9 and the figure (Figure 2) allow comparing the individual adsorption working pairs. Nevertheless, the attention should also be paid to the differences in the construction of the individual systems. The systems studied in the laboratory are very often characterised using a monolayer of adsorbent, whereas the real ones are packed beds. Therefore, in the case of adsorption beds with several layers of adsorbent, both adsorption and desorption take longer, and this is another criterion that, besides the heat transfer coefficient between adsorbent and bed, affects the performance of the system and requires several analyses.

The discussed studies included analyses of the duration and values of the individual temperatures of the adsorption chiller operating cycle. It should be stated that the common point of the discussed studies is the need for further research in real operating conditions. Modi et al. [101] in their study analysed solar heat as an energy source for adsorbent bed regeneration. The system studied was operated with AC35/methanol vapour, and the researchers determined the effect of actual ambient conditions on cooling performance. It was found that a temperature of 100 °C is the value for which the efficiency of the operating process is the highest. In addition, it was found that actual operating conditions generate a decrease in ice production efficiency and COP of about 30%. This value is related to the conditions in India, which also allows analysing the profitability of the investment. On this basis, the payback time of the 9.25 kW adsorption system was determined to be 3.5 years, with an annual reduction in CO<sub>2</sub> emissions of almost 13 tonnes. However, it is not easy to estimate the overall annual cost of operation of individual solutions, due to the variety of cooler design options. The choice of a specific adsorption working pair influences the amount of heat necessary for bed regeneration and the amount of energy consumed by the vacuum pump that ensures the right bed pressure for the application. Therefore, the annual operating cost of an adsorption chiller is based on the amount of electricity consumed by the vacuum pump, circulating pump, and control systems, and thus the annual operating cost is based on the price of electricity in the region. Of course, it is also necessary to analyse the demand for cooling, to assess whether this demand is constant or variable throughout the day, because all this affects the operating costs. Obviously, for a given chiller and a particular adsorption working pair, the highest operating costs will be for freezing and the lowest for air conditioning. The final annual cost of operating an adsorption chiller depends on the location of the application, electricity prices, the amount of refrigeration demand, the specific application, the source of the bed regeneration heat, and the chiller design in general.

Analysing publications on adsorption systems driven by solar heat, it can be stated that they are mostly based on classical working pairs and are characterised by low SCP values. Nevertheless, most publications on real adsorption systems are based on solar heat as the driving energy. Furthermore, studies focusing on the optimisation of adsorption and desorption times also mostly refer to these systems. This has to do with the characteristics of solar radiation, which is time-varying, affecting the temperature fluctuations of the desorption heat. In addition, the cooling load is also characterised by a variation in demand throughout the day. On this basis, it can be concluded that solar-powered adaptive temporary adsorption chillers will continue to be the subject of further research, as they are already in use in India, for example, and further modifications can only accelerate their wider application, especially in the African, Asian, and Central American regions. It should also be noted that among the solutions discussed, adsorption working pairs operating with a refrigerant evaporation temperature of 0–10 °C predominate, which allows them to be classified in the group of refrigeration or air conditioning solutions. Thus, it can be concluded that the use of adsorption cycle in freezing requires much research and analysis, as it has not received much attention in contemporary research.

Generally, current research focuses on the use of composite adsorbents and MOFs. MOFs are now a very widely researched group of materials because they allow the production of materials with specific parameters that are beneficial for a given application,

although the disadvantages of these materials are the high price and the need to analyse the stability and durability of the newly developed MOFs. Nevertheless, further development of classical adsorbent/adsorbate pairs is also observed. Analyzing solutions based on physical adsorbents, it was found that their main advantages are easy availability, relatively low price, and the ability to operate at desorption temperatures of 40–50 °C. On the other hand, these adsorbents are already very well studied and in their original form prevent further improvement of the COP and SCP performance of the chiller. However, this group of materials provides a basis for the development of another one, which are composite and doped adsorbents. Their main advantage is the ability to shape the properties of the adsorbent formed. The use of different additives allows for improving heat and mass transport in the adsorption bed. On the other hand, the disadvantage of this group of adsorbents is the need to analyse the effect of doping on the clogging of pores in the adsorbent.

The most important conclusion from the analysis of the adsorption coating studies is that the use of an adsorption coating compared to a packed bed results in an intensification of heat and mass transport in the bed. The cited results indicate an increase of up to 500% in SCP values for the coated bed compared to the packed bed. In the case of COP, two trends of change were found, i.e., an increase up to 70% and a decrease up to 60%. However, it should be noted that the number of tests carried out for different configurations of the bed structure under comparable conditions is small, so further studies of coated beds are needed to verify contradictions in the results obtained.

Most studies of adsorbent coatings consider SG/water working pairs' application. However, comparative studies of coatings consisting of different adsorbents are lacking. These studies would give an idea of how the different materials interact with the binders.

Among the studies cited on the preparation of adsorption coatings, the immersion technique was most commonly used, due to the simplicity of obtaining the appropriate adsorbent/binder mixture. In contrast, the number of studies of coatings obtained by in situ methods is small. The main reasons for this are the high technological requirements, including high process temperature and pressure, and the small difference in performance improvement of the adsorption cooling system compared to ex situ methods.

An analysis of the influence of basic coating design parameters on heat and mass transport was carried out. A decrease in the SCP value of the system was observed with increasing coating thickness. The occurrence of optimum thickness depending on conditions and COP values was found. From the point of view of the adsorption process, it is more advantageous to use larger adsorbent particles as a coating component and to aim to minimise the proportion of binder. Potential research within the framework of parameters selection for the construction of adsorption coatings should be particularly directed towards the development of technology for obtaining coatings with variable proportion and gradient of porosity, as appropriate adjustment of these parameters allows improvement of SCP values.

The main challenge of the following publications is that there are few studies of different adsorption working pairs conducted under the same conditions (temperature values and heat exchanger type). The simulation studies also require careful analysis, due to the fact that CFD simulations conducted very often use as input data experimental measurements of other researchers, which were conducted under very specific conditions. Using the results data under even slightly changed operating conditions and developing a series of new simulation measurements can be misleading and lead to error propagation.

Analysing the objectives of individual papers, it can be concluded that they boil down to increasing the energy efficiency of the adsorption cooling cycle, which can be achieved by developing better adsorbents, selecting an appropriate adsorption working pair and using adsorbent to coat elements of the bed structure. However, presentation of COP and SCP parameters for a given adsorption working pair as a conclusion from the research carried out, without specifying the conditions under which these parameters were obtained, makes it much more difficult to conduct further analyses involving research in real operating conditions.

The results presented in this paper from different authors show a great diversity in experimental approach, adsorbents, adsorbates, binders, and operating parameters used. Therefore, there are still many different combinations of the above mentioned to be investigated, which will contribute to the further development of adsorption refrigeration.

## 6. Conclusions

Analysing recent works, many different experimental approaches in the field of adsorption cooling can be observed. This fact makes it difficult to compare the results presented by different authors. Therefore, it has to be concluded that the knowledge on the applications of different adsorption working pairs and coatings is incomplete.

Adsorption chillers are mostly studied for adsorbate evaporation temperatures in the range of 0–15 °C with water as refrigerant. The number of works considering the application of adsorption chillers in freezing is negligible, and the available studies describe solutions using methanol and ethanol as adsorbates. Among the works analysed, the application of most of the working pairs allows for obtaining a SCP < 500 W/kg and COP < 0.6. Only MOFs/water pairs achieve the desired high COP > 0.6 at SCP > 800 W/kg. For many pairs, a high COP is obtained with relatively low SCP < 300 W/kg, leading to increased bed dimensions and thus application problems. MOFs are up to 15 times better than classical working pairs with activated carbons or silica gels, which compensates for the difference in price of these adsorbents. For zeolite/methanol pairs, the application of bed coating allows up to a 5-times increase in SCP, with a 25% increase in COP, which allows to state that further development of classical adsorbents is possible. In the case of MOF/water pairs, the coating allows to increase SCP by 2.5 times and COP by up to 30%. Most of the discussed works focus on coatings thicker than 100 µm, which is connected to dip coating technique. In order to obtain thinner coatings with thicknesses of several microns, the in situ method should be used.

Summarising the collected observations, it should be stated that the modifications related to the adsorption working pair allow for a significant intensification of the heat and mass transfer in the bed, thus improving the COP and SCP coefficients. When considering potential trends for further research, according to the authors, the possibility of using mixtures of multicomponent adsorbents and mixtures of various natural refrigerants should be analysed. Further development of in-situ coatings in combination with MOF adsorbents could be an important step towards improving the efficiency of adsorption systems.

The analysis of the various adsorbates, adsorbents, adsorbent coatings, and operating temperatures used in refrigerators carried out in this work allows us to conclude that there are still opportunities for development in this field. In addition, it should be noted that each combination of the above-mentioned elements and parameters corresponds to an individual sorption curve. On this basis, the authors decided to draw attention to the need for detailed guidelines for testing adsorption chillers, analogous to those for heat pumps. Therefore, each adsorption working pair should be characterised by a set of COP and SCP parameters, determined for characteristic (e.g., 18) measurement points:  $T_{\text{ads}} = 30 \text{ °C}$ ,  $T_{\text{des}} = \{60; 90; 120 \text{ °C}\}$  and  $T_{\text{eva}} = \{+12; +7; +2; -2; -7; -15 \text{ °C}\}$ . The use of this system objectifies the evaluation of adsorption chillers, allows comparison of bed materials, and is an opportunity for significant progress in the development of the adsorption chiller industry.

Furthermore, tests conducted under real conditions, including heat losses and possible desorption temperature fluctuations (e.g.,  $\pm 10 \text{ °C}$ ), are necessary for proper evaluation of adsorption chillers. On the basis of the presented test results, it can be concluded that it is possible both to use environmentally friendly working vapours in the device and to use waste energy or renewable energy sources for its powering (low bed regeneration temperature), which will obtain relatively high values of COP and SCP coefficients.

**Author Contributions:** The co-authors contribution to the paper was: conceptualisation, P.B. and T.B.; formal analysis, Ł.M. and K.S.; writing—original draft preparation, P.B. and T.B.; writing—review and editing, Ł.M. and K.S.; visualisation, Ł.M., K.S., P.B. and T.B.; supervision, Ł.M. and K.S.; funding acquisition, Ł.M. and K.S. All authors have read and agreed to the published version of the manuscript.

**Funding:** The paper was funded by government money Department of Energy and Fuels number 16.16.210.476 (research subsidy).

**Data Availability Statement:** Not applicable.

**Conflicts of Interest:** The authors declare no conflict of interest.

## Nomenclature

|                    |                               |
|--------------------|-------------------------------|
| $T_{\text{eva}}$   | evaporation temperature, °C   |
| $T_{\text{chill}}$ | cooling water temperature, °C |
| $T_{\text{heat}}$  | heating water temperature, °C |
| $T_{\text{ads}}$   | adsorption temperature, °C    |
| $T_{\text{des}}$   | desorption temperature, °C    |

## Abbreviations

|       |   |
|-------|---|
| AA    | anodic alumina                                    |
| AC    | activated carbon                                  |
| ACF   | activated carbon fiber                            |
| COP   | coefficient of performance                        |
| EG    | expanded graphite                                 |
| GNP   | graphene nanoplatelet                             |
| GWP   | global warming potential                          |
| HDACF | high-density activated carbon fibre               |
| HEC   | hydroxyethylcellulose                             |
| IUPAC | International Union of Pure and Applied Chemistry |
| MOF   | metal organic framework                           |
| ODP   | ozone depletion potential                         |
| PTFE  | polytetrafluoroethylene                           |
| PVA   | polyvinyl alcohol                                 |
| PVP   | polyvinyl pyrrolidone                             |
| SCP   | specific cooling power                            |
| SG    | silica gel  |
| SGP   | silica gel powder                                 |

## References

- International Energy Agency World Energy Balances. *World Energy Balances Overview 2019*; International Energy Agency World Energy Balances: Paris, France, 2019.
- Streck, C.; Von Unger, M.; Krämer, N. From Paris to Katowice: Cop-24 Tackles the Paris Rulebook. *J. Eur. Environ. Plan. Law* **2019**, *16*, 165–190. [[CrossRef](#)]
- Hassan, H.; Mohamad, A.; Alyousef, Y.; Al-Ansary, H. A review on the equations of state for the working pairs used in adsorption cooling systems. *Renew. Sustain. Energy Rev.* **2015**, *45*, 600–609. [[CrossRef](#)]
- Elsheniti, M.B.; Elsamni, O.A.; Al-Dadah, R.K.; Mahmoud, S.; Elsayed, E.; Saleh, K. Adsorption Refrigeration Technologies. *Sustain. Air Cond. Syst.* **2018**, 71–95. [[CrossRef](#)]
- Demir, H.; Mobedi, M.; Ülkü, S. A review on adsorption heat pump: Problems and solutions. *Renew. Sustain. Energy Rev.* **2008**, *12*, 2381–2403. [[CrossRef](#)]
- Council of European Energy Regulators (CEER). *Report on Power Losses 2017*; Council of European Energy Regulators (CEER): Brussels, Belgium, 2017.
- Sztekler, K.; Kalawa, W.; Nowak, W.; Mika, L.; Gradziel, S.; Krzywanski, J.; Radoska, E. Experimental Study of Three-Bed Adsorption Chiller with Desalination Function. *Energies* **2020**, *13*, 5827. [[CrossRef](#)]
- Sztekler, K.; Kalawa, W.; Mika, Ł.; Mlonka-Medrala, A.; Sowa, M.; Nowak, W. Effect of Additives on the Sorption Kinetics of a Silica Gel Bed in Adsorption Chiller. *Energies* **2021**, *14*, 1083. [[CrossRef](#)]

9. Thommes, M.; Kaneko, K.; Neimark, A.V.; Olivier, J.P.; Rodriguez-Reinoso, F.; Rouquerol, J.; Sing, K.S.W. Physisorption of gases, with special reference to the evaluation of surface area and pore size distribution (IUPAC Technical Report). *Pure Appl. Chem.* **2015**, *87*, 1051–1069. [CrossRef]
10. European Union Council Decision (EU). 2017/1541 of 17 July 2017—on the Conclusion, on Behalf of the European Union, of the Kigali Amendment to the Montreal Protocol on Substances That Deplete the Ozone Layer. *Off. J. Eur. Union* **2017**, *L 236*, 1–2.
11. Engineering ToolBox. 2001. Available online: <https://www.engineeringtoolbox.com> (accessed on 24 April 2021).
12. Engineering ToolBox. Argon—Density and Specific Weight. 2018. Available online: [https://www.engineeringtoolbox.com/argon-density-specific-weight-temperature-pressure-d\\_2089.html](https://www.engineeringtoolbox.com/argon-density-specific-weight-temperature-pressure-d_2089.html) (accessed on 24 April 2021).
13. Allouhi, A.; Kousksou, T.; Jamil, A.; El Rhafiki, T.; Mourad, Y.; Zeraouli, Y. Optimal working pairs for solar adsorption cooling applications. *Energy* **2015**, *79*, 235–247. [CrossRef]
14. Ojha, M.K.; Shukla, A.K.; Verma, P.; Kannojiya, R. Recent progress and outlook of solar adsorption refrigeration systems. In *Proceedings of the Materials Today*; Elsevier BV: Amsterdam, The Netherlands, 2020.
15. Wang, R.; Wang, L.; Wu, J. *Adsorption Refrigeration Technology*; Wiley: Hoboken, NJ, USA, 2014.
16. Sharma, R.; Kumar, E.A. Performance evaluation of simple and heat recovery adsorption cooling system using measured NH<sub>3</sub> sorption characteristics of halide salts. *Appl. Therm. Eng.* **2017**, *119*, 459–471. [CrossRef]
17. Jiang, L.; Lu, Y.; Tang, K.; Roskilly, A.P.; Wang, Y.; Yuan, Y.; Wang, R.; Wang, L. Investigation of a novel composite sorbent for improved sorption characteristic. *Energy Procedia* **2017**, *142*, 1455–1461. [CrossRef]
18. Boman, D.; Hoysall, D.C.; Pahinkar, D.G.; Ponkala, M.J.; Garimella, S. Screening of working pairs for adsorption heat pumps based on thermodynamic and transport characteristics. *Appl. Therm. Eng.* **2017**, *123*, 422–434. [CrossRef]
19. Chan, K.C.; Tso, C.Y.; Wu, C.; Chao, C.Y. Enhancing the performance of a zeolite 13X/CaCl<sub>2</sub>–water adsorption cooling system by improving adsorber design and operation sequence. *Energy Build.* **2018**, *158*, 1368–1378. [CrossRef]
20. Grekova, A.; Girkov, I.; Nikulin, V.; Tokarev, M.; Gordeeva, L.; Aristov, Y. New composite sorbents of water and methanol “salt in anodic alumina”: Evaluation for adsorption heat transformation. *Energy* **2016**, *106*, 231–239. [CrossRef]
21. Brancato, V.; Frazzica, A.; Sapienza, A.; Gordeeva, L.; Freni, A. Ethanol adsorption onto carbonaceous and composite adsorbents for adsorptive cooling system. *Energy* **2015**, *84*, 177–185. [CrossRef]
22. Dzigbor, A.; Chimphango, A. Evaluating the potential of using ethanol/water mixture as a refrigerant in adsorption cooling system by using activated carbon—sodium chloride composite adsorbent. *Int. J. Refrig.* **2019**, *97*, 132–142. [CrossRef]
23. Dias, J.M.; Costa, V.A. Adsorption heat pumps for heating applications: A review of current state, literature gaps and development challenges. *Renew. Sustain. Energy Rev.* **2018**, *98*, 317–327. [CrossRef]
24. Kumita, M.; Yamawaki, N.; Shinohara, K.; Higashi, H.; Kodama, A.; Kobayashi, N.; Seto, T.; Otani, Y. Methanol adsorption behaviors of compression-molded activated carbon fiber with PTFE. *Int. J. Refrig.* **2018**, *94*, 127–135. [CrossRef]
25. Mitra, S.; Muttakin, M.; Thu, K.; Saha, B.B. Study on the influence of adsorbent particle size and heat exchanger aspect ratio on dynamic adsorption characteristics. *Appl. Therm. Eng.* **2018**, *133*, 764–773. [CrossRef]
26. Rupam, T.; Islam, A.; Pal, A.; Saha, B.B. Adsorption thermodynamics and performance indicators of selective adsorbent/refrigerant pairs. *Appl. Therm. Eng.* **2020**, *175*, 115361. [CrossRef]
27. Palomba, V.; Vasta, S.; Giacoppo, G.; Calabrese, L.; Gulli, G.; La Rosa, D.; Freni, A. Design of an Innovative Graphite Exchanger for Adsorption Heat Pumps and Chillers. *Energy Procedia* **2015**, *81*, 1030–1040. [CrossRef]
28. Frazzica, A.; Palomba, V.; Dawoud, B.; Gulli, G.; Brancato, V.; Sapienza, A.; Vasta, S.; Freni, A.; Costa, F.; Restuccia, G. Design, realization and testing of an adsorption refrigerator based on activated carbon/ethanol working pair. *Appl. Energy* **2016**, *174*, 15–24. [CrossRef]
29. Brancato, V.; Gordeeva, L.; Sapienza, A.; Freni, A.; Frazzica, A. Dynamics study of ethanol adsorption on microporous activated carbon for adsorptive cooling applications. *Appl. Therm. Eng.* **2016**, *105*, 28–38. [CrossRef]
30. Singh, V.K.; Kumar, E.A.; Saha, B.B. Adsorption isotherms, kinetics and thermodynamic simulation of CO<sub>2</sub>-CSAC pair for cooling application. *Energy* **2018**, *160*, 1158–1173. [CrossRef]
31. Singh, V.K.; Kumar, E.A. Thermodynamic analysis of single-stage and single-effect two-stage adsorption cooling cycles using indigenous coconut shell based activated carbon-CO<sub>2</sub> pair. *Int. J. Refrig.* **2017**, *84*, 238–252. [CrossRef]
32. Girkov, I.; Okunev, B.; Aristov, Y. Dynamics of pressure- and temperature-initiated adsorption cycles for transformation of low temperature heat: Flat bed of loose grains. *Appl. Therm. Eng.* **2020**, *165*, 114654. [CrossRef]
33. Hamrahi, S.E.; Goudarzi, K.; Yaghoubi, M. Experimental study of the performance of a continuous solar adsorption chiller using Nano-activated carbon/methanol as working pair. *Sol. Energy* **2018**, *173*, 920–927. [CrossRef]
34. Yaïci, W.; Entchev, E. Coupled unsteady computational fluid dynamics with heat and mass transfer analysis of a solar/heat-powered adsorption cooling system for use in buildings. *Int. J. Heat Mass Transf.* **2019**, *144*, 118648. [CrossRef]
35. Vodianitskaia, P.J.; Soares, J.J.; Melo, H.; Gurgel, J.M. Experimental chiller with silica gel: Adsorption kinetics analysis and performance evaluation. *Energy Convers. Manag.* **2017**, *132*, 172–179. [CrossRef]
36. Mohammed, R.H.; Mesalhy, O.; Elsayed, M.L.; Hou, S.; Su, M.; Chow, L.C. Physical properties and adsorption kinetics of silica-gel/water for adsorption chillers. *Appl. Therm. Eng.* **2018**, *137*, 368–376. [CrossRef]
37. Mohammed, R.H.; Mesalhy, O.; Elsayed, M.L.; Chow, L.C. Performance evaluation of a new modular packed bed for adsorption cooling systems. *Appl. Therm. Eng.* **2018**, *136*, 293–300. [CrossRef]

38. Hong, S.W.; Ahn, S.H.; Chung, J.D.; Bae, K.J.; Cha, D.A.; Kwon, O.K. Characteristics of FAM-Z01 compared to silica gels in the performance of an adsorption bed. *Appl. Therm. Eng.* **2016**, *104*, 24–33. [[CrossRef](#)]
39. Li, M.; Zhao, Y.; Long, R.; Liu, Z.; Liu, W. Computational fluid dynamic study on adsorption-based desalination and cooling systems with stepwise porosity distribution. *Desalination* **2021**, *508*, 115048. [[CrossRef](#)]
40. Seol, S.-H.; Nagano, K.; Togawa, J. Modeling of adsorption heat pump system based on experimental estimation of heat and mass transfer coefficients. *Appl. Therm. Eng.* **2020**, *171*, 115089. [[CrossRef](#)]
41. Liu, Y.; Yuan, Z.; Wen, X.; Du, C. Evaluation on performance of solar adsorption cooling of silica gel and SAPO-34 zeolite. *Appl. Therm. Eng.* **2021**, *182*, 116019. [[CrossRef](#)]
42. Radu, A.; Defraeye, T.; Ruch, P.; Carmeliet, J.; Derome, D. Insights from modeling dynamics of water sorption in spherical particles for adsorption heat pumps. *Int. J. Heat Mass Transf.* **2017**, *105*, 326–337. [[CrossRef](#)]
43. Kayal, S.; Baichuan, S.; Saha, B. Adsorption characteristics of AQSOA zeolites and water for adsorption chillers. *Int. J. Heat Mass Transf.* **2016**, *92*, 1120–1127. [[CrossRef](#)]
44. Girmik, I.; Grekova, A.; Gordeeva, L.; Aristov, Y. Dynamic optimization of adsorptive chillers: Compact layer vs. bed of loose grains. *Appl. Therm. Eng.* **2017**, *125*, 823–829. [[CrossRef](#)]
45. Girmik, I.S.; Aristov, Y. Dynamics of water vapour adsorption by a monolayer of loose AQSOA™-FAM-Z02 grains: Indication of inseparably coupled heat and mass transfer. *Energy* **2016**, *114*, 767–773. [[CrossRef](#)]
46. Teo, H.W.B.; Chakraborty, A.; Han, B. Water adsorption on CHA and AFI types zeolites: Modelling and investigation of adsorption chiller under static and dynamic conditions. *Appl. Therm. Eng.* **2017**, *127*, 35–45. [[CrossRef](#)]
47. Kim, S.H.; Cho, K.; Kim, J.-N.; Beum, H.T.; Yoon, H.C.; Lee, C.H. Improvement of cooling performance of water adsorption chiller by using aluminophosphate adsorbent. *Microporous Mesoporous Mater.* **2020**, *309*, 110572. [[CrossRef](#)]
48. Fan, W.; Chakraborty, A. Isothermic heat of adsorption at zero coverage for AQSOA-Z01/Z02/Z05 zeolites and water systems. *Microporous Mesoporous Mater.* **2018**, *260*, 201–207. [[CrossRef](#)]
49. Wang, S.; Xia, X.; Li, S. Cooling performance of metal organic framework-water pairs in cascaded adsorption chillers. *Appl. Therm. Eng.* **2021**, *189*, 116707. [[CrossRef](#)]
50. Shmroukh, A.N.; Ali, A.H.H.; Ookawara, S. Adsorption working pairs for adsorption cooling chillers: A review based on adsorption capacity and environmental impact. *Renew. Sustain. Energy Rev.* **2015**, *50*, 445–456. [[CrossRef](#)]
51. Han, B.; Chakraborty, A. Adsorption characteristics of methyl-functional ligand MOF-801 and water systems: Adsorption chiller modelling and performances. *Appl. Therm. Eng.* **2020**, *175*, 115393. [[CrossRef](#)]
52. Ma, L.; Rui, Z.; Wu, Q.; Yang, H.; Yin, Y.; Liu, Z.; Cui, Q.; Wang, H. Performance evaluation of shaped MIL-101-ethanol working pair for adsorption refrigeration. *Appl. Therm. Eng.* **2016**, *95*, 223–228. [[CrossRef](#)]
53. Solovyeva, M.V.; Aristov, Y.; Gordeeva, L.G. NH<sub>2</sub>-MIL-125 as promising adsorbent for adsorptive cooling: Water adsorption dynamics. *Appl. Therm. Eng.* **2017**, *116*, 541–548. [[CrossRef](#)]
54. Gordeeva, L.G.; Tu, Y.D.; Pan, Q.; Palash, M.; Saha, B.B.; Aristov, Y.I.; Wang, R.Z. Metal-organic frameworks for energy conversion and water harvesting: A bridge between thermal engineering and material science. *Nano Energy* **2021**, *84*, 105946. [[CrossRef](#)]
55. Karmakar, A.; Prabakaran, V.; Zhao, D.; Chua, K.J. A review of metal-organic frameworks (MOFs) as energy-efficient desiccants for adsorption driven heat-transformation applications. *Appl. Energy* **2020**, *269*, 115070. [[CrossRef](#)]
56. Youssef, P.; Mahmoud, S.; Al-Dadah, R.; Elsayed, E.; Elsamni, O. Numerical Investigation of Aluminum Fumarate MOF adsorbent material for adsorption desalination/cooling application. *Energy Procedia* **2017**, *142*, 1693–1698. [[CrossRef](#)]
57. Solovyeva, M.; Gordeeva, L.; Krieger, T.; Aristov, Y. MOF-801 as a promising material for adsorption cooling: Equilibrium and dynamics of water adsorption. *Energy Convers. Manag.* **2018**, *174*, 356–363. [[CrossRef](#)]
58. Younes, M.M.; El-Sharkawy, I.I.; Kabeel, A.; Uddin, K.; Miyazaki, T.; Saha, B.B. Characterization of silica gel-based composites for adsorption cooling applications. *Int. J. Refrig.* **2020**, *118*, 345–353. [[CrossRef](#)]
59. Yagnamurthy, S.; Rakshit, D.; Jain, S.; Rocky, K.A.; Islam, A.; Saha, B.B. Adsorption of difluoromethane onto activated carbon based composites: Thermophysical properties and adsorption characterization. *Int. J. Heat Mass Transf.* **2021**, *171*, 121112. [[CrossRef](#)]
60. Pal, A.; Uddin, K.; Rocky, K.A.; Thu, K.; Saha, B.B. CO<sub>2</sub> adsorption onto activated carbon-graphene composite for cooling applications. *Int. J. Refrig.* **2019**, *106*, 558–569. [[CrossRef](#)]
61. Chen, Q.; Du, S.; Yuan, Z.; Sun, T.; Li, Y. Experimental study on performance change with time of solar adsorption refrigeration system. *Appl. Therm. Eng.* **2018**, *138*, 386–393. [[CrossRef](#)]
62. Wang, Q.; Gao, X.; Xu, J.; Maiga, A.; Chen, G. Experimental investigation on a fluidized-bed adsorber/desorber for the adsorption refrigeration system. *Int. J. Refrig.* **2012**, *35*, 694–700. [[CrossRef](#)]
63. Younes, M.M.; El-Sharkawy, I.I.; Kabeel, A.E.; Uddin, K.; Pal, A.; Mitra, S.; Thu, K.; Saha, B.B. Synthesis and characterization of silica gel composite with polymer binders for adsorption cooling applications. *Int. J. Refrig.* **2019**, *98*, 161–170. [[CrossRef](#)]
64. Qadir, N.U.; Said, S.A.; Ben Mansour, R. Modeling the performance of a two-bed solar adsorption chiller using a multi-walled carbon nanotube/MIL-100(Fe) composite adsorbent. *Renew. Energy* **2017**, *109*, 602–612. [[CrossRef](#)]
65. Kim, D.-S.; Chang, Y.-S.; Lee, D.-Y. Modelling of an adsorption chiller with adsorbent-coated heat exchangers: Feasibility of a polymer-water adsorption chiller. *Energy* **2018**, *164*, 1044–1061. [[CrossRef](#)]
66. Ammann, J.; Michel, B.; Ruch, P.W. Characterization of transport limitations in SAPO-34 adsorbent coatings for adsorption heat pumps. *Int. J. Heat Mass Transf.* **2019**, *129*, 18–27. [[CrossRef](#)]

67. Grabowska, K.; Sosnowski, M.; Krzywanski, J.; Sztেকler, K.; Kalawa, W.; Zylka, A.; Nowak, W. Analysis of heat transfer in a coated bed of an adsorption chiller. *MATEC Web Conf.* **2018**, *240*, 01010. [[CrossRef](#)]
68. Freni, A.; Bonaccorsi, L.; Calabrese, L.; Capri, A.; Frazzica, A.; Sapienza, A. SAPO-34 coated adsorbent heat exchanger for adsorption chillers. *Appl. Therm. Eng.* **2015**, *82*, 1–7. [[CrossRef](#)]
69. Chang, K.-S.; Chen, M.-T.; Chung, T.-W. Effects of the thickness and particle size of silica gel on the heat and mass transfer performance of a silica gel-coated bed for air-conditioning adsorption systems. *Appl. Therm. Eng.* **2005**, *25*, 2330–2340. [[CrossRef](#)]
70. Restuccia, G.; Freni, A.; Russo, F.; Vasta, S. Experimental investigation of a solid adsorption chiller based on a heat exchanger coated with hydrophobic zeolite. *Appl. Therm. Eng.* **2005**, *25*, 1419–1428. [[CrossRef](#)]
71. Restuccia, G.; Freni, A.; Maggio, G. A zeolite-coated bed for air conditioning adsorption systems: Parametric study of heat and mass transfer by dynamic simulation. *Appl. Therm. Eng.* **2002**, *22*, 619–630. [[CrossRef](#)]
72. Seol, S.-H.; Nagano, K.; Togawa, J. A new experimental method to separate interfacial and internal mass transfer on coated adsorbent. *Appl. Therm. Eng.* **2019**, *159*, 113869. [[CrossRef](#)]
73. Kumita, M.; Oya, T.; Matsui, K.; Suwa, Y.; Kodama, A.; Higashi, H.; Seto, T.; Otani, Y. Deposition of thick, rigid and size-controlled silica particle layer on aluminum sheet for water vapor adsorption. *Appl. Therm. Eng.* **2017**, *124*, 815–819. [[CrossRef](#)]
74. Li, A.; Thu, K.; Bin Ismail, A.; Shahzad, M.W.; Ng, K.C. Performance of adsorbent-embedded heat exchangers using binder-coating method. *Int. J. Heat Mass Transf.* **2016**, *92*, 149–157. [[CrossRef](#)]
75. Wang, L.; Bu, X.; Ma, W. Experimental study of an Adsorption Refrigeration Test Unit. *Energy Procedia* **2018**, *152*, 895–903. [[CrossRef](#)]
76. Kummer, H.; Földner, G.; Henninger, S.K. Versatile siloxane based adsorbent coatings for fast water adsorption processes in thermally driven chillers and heat pumps. *Appl. Therm. Eng.* **2015**, *85*, 1–8. [[CrossRef](#)]
77. Pinheiro, J.M.; Salústio, S.; Geraldes, V.; Valente, A.A.; Silva, C.M. Copper foam coated with CPO-27(Ni) metal–organic framework for adsorption heat pump: Simulation study using OpenFOAM. *Appl. Therm. Eng.* **2020**, *178*, 115498. [[CrossRef](#)]
78. Pahinkar, D.G.; Boman, D.B.; Garimella, S. High performance microchannel adsorption heat pumps. *Int. J. Refrig.* **2020**, *119*, 184–194. [[CrossRef](#)]
79. Albaik, I.; Al-Dadah, R.; Mahmoud, S.; Almesfer, M.K.; Ismail, M.A.; Elsayed, E.; Saleh, M. A comparison between the packed and coated finned tube for adsorption system using aluminium fumarate: Numerical study. *Therm. Sci. Eng. Prog.* **2021**, *22*, 100859. [[CrossRef](#)]
80. Duong, X.Q.; Cao, N.V.; Lee, W.S.; Park, M.Y.; Chung, J.D.; Bae, K.J.; Kwon, O.K. Effect of coating thickness, binder and cycle time in adsorption cooling applications. *Appl. Therm. Eng.* **2021**, *184*, 116265. [[CrossRef](#)]
81. Sztেকler, K.; Kalawa, W.; Mlonka-Medrala, A.; Nowak, W.; Mika, Ł.; Krzywanski, J.; Grabowska, K.; Sosnowski, M.; Debniak, M. The Effect of Adhesive Additives on Silica Gel Water Sorption Properties. *Entropy* **2020**, *22*, 327. [[CrossRef](#)]
82. McCague, C.; Huttema, W.; Fradin, A.; Bahrami, M. Lab-scale sorption chiller comparison of FAM-Z02 coating and pellets. *Appl. Therm. Eng.* **2020**, *173*, 115219. [[CrossRef](#)]
83. Rezk, A.; Al-Dadah, R.; Mahmoud, S.; Elsayed, A. Effects of contact resistance and metal additives in finned-tube adsorbent beds on the performance of silica gel/water adsorption chiller. *Appl. Therm. Eng.* **2013**, *53*, 278–284. [[CrossRef](#)]
84. Wittstadt, U.; Földner, G.; Laurenz, E.; Warlo, A.; Große, A.; Herrmann, R.; Schnabel, L.; Mittelbach, W. A novel adsorption module with fiber heat exchangers: Performance analysis based on driving temperature differences. *Renew. Energy* **2017**, *110*, 154–161. [[CrossRef](#)]
85. Sapienza, A.; Gulli, G.; Calabrese, L.; Palomba, V.; Frazzica, A.; Brancato, V.; La Rosa, D.; Vasta, S.; Freni, A.; Bonaccorsi, L.; et al. An innovative adsorptive chiller prototype based on 3 hybrid coated/granular adsorbents. *Appl. Energy* **2016**, *179*, 929–938. [[CrossRef](#)]
86. Ouchi, T.; Hamamoto, Y.; Mori, H.; Takata, S.; Etoh, A. Water vapor adsorption equilibrium and adsorption/desorption rate of porous alumina film adsorbent synthesized with anodization on heat transfer plate. *Appl. Therm. Eng.* **2014**, *72*, 219–228. [[CrossRef](#)]
87. Tatlier, M.; Kummer, H.; Henninger, S.K. Crystallization of zeolite X coatings on stainless steel by microwave heating. *J. Porous Mater.* **2015**, *22*, 347–352. [[CrossRef](#)]
88. Capri, A.; Frazzica, A.; Calabrese, L. Recent Developments in Coating Technologies for Adsorption Heat Pumps: A Review. *Coatings* **2020**, *10*, 855. [[CrossRef](#)]
89. Dias, J.M.; Costa, V.A. Evaluating the performance of a coated tube adsorber for adsorption cooling. *Int. J. Refrig.* **2020**, *118*, 21–30. [[CrossRef](#)]
90. Frazzica, A.; Földner, G.; Sapienza, A.; Freni, A.; Schnabel, L. Experimental and theoretical analysis of the kinetic performance of an adsorbent coating composition for use in adsorption chillers and heat pumps. *Appl. Therm. Eng.* **2014**, *73*, 1022–1031. [[CrossRef](#)]
91. Bahremand, H.; Ahmadi, M.; Bahrami, M. Analytical modeling of oscillatory heat transfer in coated sorption beds. *Int. J. Heat Mass Transf.* **2018**, *121*, 1–9. [[CrossRef](#)]
92. Li, M.; Zhao, Y.; Long, R.; Liu, Z.; Liu, W. Gradient porosity distribution of adsorbent bed for efficient adsorption cooling. *Int. J. Refrig.* **2021**, *128*, 153–162. [[CrossRef](#)]
93. Younes, M.M.; El-Sharkawy, I.I.; Kabeel, A.; Saha, B. A review on adsorbent-adsorbate pairs for cooling applications. *Appl. Therm. Eng.* **2017**, *114*, 394–414. [[CrossRef](#)]

94. Goyal, P.; Baredar, P.; Mittal, A.; Siddiqui, A.R. Adsorption refrigeration technology—An overview of theory and its solar energy applications. *Renew. Sustain. Energy Rev.* **2016**, *53*, 1389–1410. [[CrossRef](#)]
95. Shabir, F.; Sultan, M.; Miyazaki, T.; Saha, B.B.; Askalany, A.; Ali, D.I.; Zhou, Y.; Ahmad, R.; Shamshiri, R.R. Recent updates on the adsorption capacities of adsorbent-adsorbate pairs for heat transformation applications. *Renew. Sustain. Energy Rev.* **2020**, *119*, 109630. [[CrossRef](#)]
96. Papakokinos, G.; Castro, J.; López, J.; Oliva, A. A generalized computational model for the simulation of adsorption packed bed reactors—Parametric study of five reactor geometries for cooling applications. *Appl. Energy* **2019**, *235*, 409–427. [[CrossRef](#)]
97. Palomba, V.; Nowak, S.; Dawoud, B.; Frazzica, A. Dynamic modelling of Adsorption systems: A comprehensive calibrated dataset for heat pump and storage applications. *J. Energy Storage* **2021**, *33*, 102148. [[CrossRef](#)]
98. Xu, S.; Wang, L.; Wang, R. Thermodynamic analysis of single-stage and multi-stage adsorption refrigeration cycles with activated carbon–ammonia working pair. *Energy Convers. Manag.* **2016**, *117*, 31–42. [[CrossRef](#)]
99. Dakkama, H.; Elsayed, A.; Al-Dadah, R.; Mahmoud, S.; Youssef, P. Investigation of Cascading Adsorption Refrigeration System with Integrated Evaporator-Condenser Heat Exchanger Using Different Working Pairs. *Energy Procedia* **2015**, *75*, 1496–1501. [[CrossRef](#)]
100. Ma, L.; Yang, H.; Wu, Q.; Yin, Y.; Liu, Z.; Cui, Q.; Wang, H. Study on adsorption refrigeration performance of MIL-101-isobutane working pair. *Energy* **2015**, *93*, 786–794. [[CrossRef](#)]
101. Modi, N.; Pandya, B. Integration of evacuated solar collectors with an adsorptive ice maker for hot climate region. *Energy Built Environ.* **2021**. [[CrossRef](#)]
102. Girnik, I.S.; Aristov, Y. Dynamic optimization of adsorptive chillers: The “AQSOA™-FAM-Z02—Water” working pair. *Energy* **2016**, *106*, 13–22. [[CrossRef](#)]
103. Sinha, S.; Milani, D.; Luu, M.T.; Abbas, A. Enhancing the performance of a solar-assisted adsorption chiller using advanced composite materials. *Comput. Chem. Eng.* **2018**, *119*, 406–424. [[CrossRef](#)]
104. Tso, C.; Chan, K.; Chao, C.Y.; Wu, C. Experimental performance analysis on an adsorption cooling system using zeolite 13X/CaCl<sub>2</sub> adsorbent with various operation sequences. *Int. J. Heat Mass Transf.* **2015**, *85*, 343–355. [[CrossRef](#)]
105. Elsheniti, M.B.; El-Hamid, A.A.; El-Samni, O.A.; Elsherbiny, S.; Elsayed, E. Experimental evaluation of a solar two-bed lab-scale adsorption cooling system. *Alex. Eng. J.* **2021**, *60*, 2747–2757. [[CrossRef](#)]
106. Papakokinos, G.; Castro, J.; Capdevila, R.; Damle, R. A comprehensive simulation tool for adsorption-based solar-cooled buildings—Control strategy based on variable cycle duration. *Energy Build.* **2021**, *231*, 110591. [[CrossRef](#)]
107. Chan, K.; Chao, C.Y.; Sze-To, G.; Hui, K.S. Performance predictions for a new zeolite 13X/CaCl<sub>2</sub> composite adsorbent for adsorption cooling systems. *Int. J. Heat Mass Transf.* **2012**, *55*, 3214–3224. [[CrossRef](#)]
108. Qadir, N.U.; Said, S.; Mansour, R.; Imran, H.; Khan, M. Performance comparison of a two-bed solar-driven adsorption chiller with optimal fixed and adaptive cycle times using a silica gel/water working pair. *Renew. Energy* **2020**, *149*, 1000–1017. [[CrossRef](#)]
109. Velte, A.; Földner, G.; Laurenz, E.; Schnabel, L. Advanced Measurement and Simulation Procedure for the Identification of Heat and Mass Transfer Parameters in Dynamic Adsorption Experiments. *Energies* **2017**, *10*, 1130. [[CrossRef](#)]
110. Sah, R.P.; Choudhury, B.; Das, R.K. A review on low grade heat powered adsorption cooling systems for ice production. *Renew. Sustain. Energy Rev.* **2016**, *62*, 109–120. [[CrossRef](#)]
111. Rogala, Z. Adsorption chiller using flat-tube adsorbent—Performance assessment and optimization. *Appl. Therm. Eng.* **2017**, *121*, 431–442. [[CrossRef](#)]
112. Jribi, S.; Miyazaki, T.; Saha, B.; Koyama, S.; Maeda, S.; Maruyama, T. CFD simulation and experimental validation of ethanol adsorption onto activated carbon packed heat exchanger. *Int. J. Refrig.* **2017**, *74*, 345–353. [[CrossRef](#)]